

N73-21423

LASER SYSTEM OF EXTENDED RANGE

Contract NASW-2014

Final Report

**CASE FILE
COPY**

Principal Investigator:

Mr. Carlton G. Lehr

December 1972

Prepared for

National Aeronautics and Space Administration
Washington, D. C. 20546

Smithsonian Institution
Astrophysical Observatory
Cambridge, Massachusetts 02138

LASER SYSTEM OF EXTENDED RANGE

1150-11500-1000

Contract NASW-2014

Final Report

Principal Investigator:

Mr. Carlton G. Lehr

December 1972

Prepared for

National Aeronautics and Space Administration
Washington, D. C. 20546

Smithsonian Institution
Astrophysical Observatory
Cambridge, Massachusetts 02138

Page Intentionally Left Blank

TABLE OF CONTENTS

		<u>Page</u>
	ABSTRACT	vii
1	OVERVIEW	1
	1.1 Introduction	1
	1.2 Characteristics of the System	2
	1.3 Recommendations.	4
	1.4 Discussion	6
2	DETAILS	13
	2.1 Technical Background	13
	2.2 Chronology of the Program and Associated Events.	13
	2.3 Calculations of System Performance and Comparisons with Other Systems.	14
	2.4 The Laser	17
	2.5 The Transmitter	21
	2.6 The Infrared Link	28
	2.7 The Receiver	30
	2.8 Operation and Calibration	40
	2.9 Operational Statistics	47
	2.10 Data Handling	49
3	ACKNOWLEDGMENTS	59
4	REFERENCES AND BIBLIOGRAPHY.	61
5	LIST OF PROGRESS REPORTS.	65

Page Intentionally Left Blank

ILLUSTRATIONS

		<u>Page</u>
1	SAO extended-range laser in its present configuration	10
2	McDonald ruby-laser system	10
3	SAO extended-range laser in satellite configuration	11
4	SAO ruby-laser system	12
5	The range equation for the extended-range laser system	17
6	Probability that k or more electrons are detected when the average signal strength is 15 electrons	18
7	Photograph of the laser	19
8	Diagram of the laser	20
9	The transmitter	22
10	The transmitter at night, showing the laser beam	23
11	Optical diagram of the transmitter	25
12	Hartmann mask used in setting the transmitted laser beam to minimum divergence	26
13	Fresnel pattern at 200 m from the Hartmann mask of Figure 12	27
14	Diagram of the infrared link that connects the transmitting and the receiving telescopes	29
15	The 1.5-m telescope	31
16	Optical diagram of the receiver	32
17	The offset system and the photomultiplier assembly	33
18	Single-electron distribution	35
19	Block diagram of the receiving electronics	37
20	Locations of retroreflectors and prominent lunar features for offset guiding	41
21	The lunar-ranging system	45

ILLUSTRATIONS (Cont.)

		<u>Page</u>
22	Time diagram for September 23, 1972	45
23	Diagram of the laser beam and the telescope field in the plane of their intersection	47
24	Photographs of returns with signal strengths of 2 photoelectrons or more	51
25	Residuals (from the University of Texas) as a function of epoch	57

TABLES

1	Comparative characteristics of laser systems.	8
2	Optical characteristics of retroreflectors.	9
3	Satellite ranges	9
4	Characteristics of the extended-range laser system.	15
5	Comparison of various lunar laser systems	16
6	Lunar background noise.	40
7	Lunar coordinates of the four retroreflectors on the moon and the prominent features used for offset guiding	42
8	Operational statistics	48
9	Summary of returns	50
10	Residuals for the laser returns.	56

ABSTRACT

A pulsed laser system was developed for range measurements from the earth to retroreflecting satellites at distances up to that of the moon. Although in this country and abroad, other laser systems have ranged to the moon, these systems are confined to fixed locations. The system described here differs from the others by having a transportable transmitter unit that can be moved from one location to another. This unit consists of a 0.2-m coudé refractor and a high-radiance, neodymium-glass, frequency-doubled laser that operates in a single transverse mode. It can be used for lunar or distant satellite ranging at any observatory that has a telescope with an aperture diameter of about 1.5 m for the detection of the laser return pulses. This telescope is utilized in the same manner customarily employed for the observation of celestial objects. A special photometric package and the associated electronics are provided for laser ranging.

The system was used for lunar ranging from February to September 1972. Over that period, 327 hours met the conditions for lunar ranging and for safe operation set down by an agreement with the Federal Aviation Administration. Time was requested and available from Harvard College Observatory for 186 of these hours, with the weather clear for 38 of these hours. The system was in operation and ranging on the moon for a total of 24 hours, during which time the laser was pulsed 233 times and 9 returns were obtained. The ratio of returns to pulses transmitted increased as the system was perfected and operating experience obtained. On September 23, there were six returns, all of which fitted the lunar ephemeris of Dr. Derral Mulholland of the University of Texas at Austin. These were obtained from 30 transmitted laser pulses. The conditions for lunar ranging on that night were far from ideal: A slight atmospheric haze significantly reduced the transmission of the laser beam; the main mirror of the 1.5-m telescope was due for realuminization; and the laser was operating at half energy. These conditions reduced the expected strength of the return by a factor of 15. Also, the background noise level was high because of the full moon. Therefore, if operation were to be continued, more returns per night could be expected.

LASER SYSTEM OF EXTENDED RANGE

Final Report

1. OVERVIEW

1.1 Introduction

The importance of laser ranging to distant satellites and the moon has been set forth in the Williamstown report (Kaula, 1970) and in the Earth and Ocean Physics Applications Program (EOPAP) (National Aeronautics and Space Administration, 1972). These reports stress the application of space techniques to investigations in solid-earth dynamics that are of both scientific and practical benefit. Lunar ranging is one of the potential techniques for measuring the dynamic properties of the solid earth, such as tectonic plate motion, polar motion, and perturbations in the earth's rotation. Measurements from a network of sites around the globe would provide important inputs to NASA's EOPAP program. For global coverage, there must be either a large number of systems in fixed locations or fewer fixed systems and one or more movable systems. This laser system of extended range is movable.

It is expected that laser ranging can be used to detect the relative motions of the tectonic plates that make up the earth's crust. These motions are related to the forces that cause earthquakes, tidal waves, and volcanic eruptions. Laser range measurements can also be used to measure the earth's rotational variations – its polar motion (wobble) and its changing length of day (UT1). If the measurements are made to retroreflectors on the moon, lunar librations can also be determined. In fact, these latter effects must be accounted for if the range data are to be used in the study of terrestrial phenomena.

The unique characteristic of this extended-range laser system is its single-mode laser of low beam divergence. Its other components are relatively conventional. The low beam divergence makes it possible to attain the extremely narrow transmitted beam widths needed for lunar ranging with a small transmitter aperture of 20 cm,

which in turn results in the system's easy transportability. It has been used for lunar ranging and will have additional applications once other planned satellites, such as Timation III, have been launched. As recommended in Section 1.4 below, the system should be modified to incorporate technical developments that occurred while the program was in progress. With these improvements, the laser itself would contribute an error of only 4 cm to individual range measurements.* With the 1 min^{-1} pulse-repetition interval of the modified laser, the 2-cm EOPAP accuracy objective could be met by averaging the returns obtained over a 4-min interval.

1.2 Characteristics of the System

The major components of the extended-range system are the laser, the transmitting telescope, the receiving telescope, and the electronics. Each will be described briefly.

The laser is a neodymium-glass system consisting of an oscillator and two amplifiers. The frequency of the infrared radiation at $1.06 \text{ }\mu\text{m}$ from the neodymium-glass rods is doubled to a wavelength of 530 nm, where efficient detection is possible. The neodymium ions provide a low-threshold, four-level laser system. The glass in which they are uniformly imbedded can be manufactured in large rods of good optical quality. The output beam of the laser has a radiance of $5 \times 10^{19} \text{ W m}^{-2} \text{ sr}^{-1}$.†

* If the laser were modified as recommended in Section 1.4, the resulting 30-J pulse would produce a return of $(30/20) \times 15 = 22$ electrons from the Apollo 15 retrorreflector. These electrons would be generated within a pulse whose duration is less than 3 ns between half-intensity points. Since the pulse shape can be approximated by a normal probability density curve, the formula for the range error is

$$\sigma_R = \frac{0.15 T}{N^{1/2} 2(2 \ln 2)^{1/2}} = \frac{0.06370 T}{N^{1/2}} \text{ meters} ,$$

where σ_R is the standard deviation in the range measurement for a single pulse of duration T ns and a return pulse of N photoelectrons. Hence, for the modified system with $T = 3$ and $N = 22$, the range error σ_R is 0.04 m, or 4 cm.

† It is interesting to compare this figure with the corresponding one at maximum output for the ruby-laser system at McDonald Observatory, Fort Davis, Texas; the radiance is $1/24$ that of the neodymium-glass laser. If energy rather than power is considered (and if the number of photons in the returned signal is roughly proportional to the energy), the corresponding values are $1.2 \times 10^{12} \text{ J m}^{-2} \text{ sr}^{-1}$ for the neodymium-glass laser and $6.3 \times 10^9 \text{ J m}^{-2} \text{ sr}^{-1}$ for the ruby laser — a ratio of 190.

Specifically, its measured characteristics are the following:

Wavelength	530 nm
Energy per pulse	20 J
Pulse duration	25 ns
Beam diameter	20 mm
Beam divergence*	37 arcsec
Bandwidth	0.9 nm
Repetition rate	0.2 min^{-1} (1 pulse every 5 min)

The obvious advantage of a neodymium-glass laser over a ruby laser is its high radiance. The disadvantages are the lower repetition rate and the wider bandwidth.

The transmitting telescope is a coudé refractor with an aperture diameter of 0.2 m. The telescope reduces the laser-beam divergence to 3.7 arcsec, which is near the lower limit introduced by atmospheric turbulence. On the same mount is another 0.2-m refractor for direct and offset guiding.

Antireflection coated prisms, rather than mirrors, are used as the coudé elements of the transmitter because they transmit the laser beam with high efficiency and are less susceptible to damage from its high intensity. With a coudé system, the laser beam is pointed by the telescope toward the moving celestial object in question. The laser, on which a number of sensitive internal mechanical adjustments have been made, remains in a fixed position.

In operation, the epoch of the laser's transmitted pulse is controlled by the station clock, referenced to Loran C. Not all the laser's infrared beam is converted to visual energy; part is transmitted to the receiving telescope, 237 m away, where it starts the range counter.

The receiving telescope is a 1.5-m (61-inch) reflector that has been at Agassiz Station Harvard College Observatory (HCO) since 1933. Although this telescope has an accurate offset stage, which is needed when a retroreflector on the dark side of

*The full angle containing half the transmitted energy.

the moon is being tracked, it has no declination drive; this makes lunar tracking with this instrument more difficult and less accurate than with the transmitting telescope. A photometric package consisting of a 1.2-nm interference filter, a photomultiplier tube, and a thermoelectric cooling unit is attached to the offset stage at the telescope's Newtonian focus. At this focus, the field is sufficiently wide for offset tracking and the weak returning laser beam experiences the loss of only two reflecting surfaces. The photomultiplier tube (PMT), an RCA C31034A, was selected for its quantum efficiency of greater than 20% at 530 nm and for its reasonably narrow single-electron distribution. Rather than the usual semitransparent oxide cathode, it uses a GaAs opaque cathode with a higher quantum efficiency. The small cathode area and low value of the maximum anode current of this tube created special problems in the optical design of the photometric package, but the problems were solved and the receiver operated successfully even when the moon was full and the noise background was high.*

The electronics of the system were modified as the program progressed. The 10-ns range counter originally used was replaced first with a 1-ns and later with a 0.1-ns counter. In the final configuration, ranges were measured simultaneously in two ways: with the 0.1-ns counter at a two-electron threshold level, and with the 10-ns counter and a fast oscilloscope at the single-electron threshold level. Since all return pulses were displayed on an oscilloscope and photographed, pulse amplitudes as well as transit times were obtained. The counters were driven by a quartz oscillator whose stability was 5 parts in 10^{12} over a period of 1 s.

1.3 Recommendations

In its present configuration, the system obtained returns from the moon. It can be moved to some other astronomical observatory with a 1.5-m telescope for additional lunar observations or for range measurements to the Timation III satellite, to a geostationary satellite, or to any other object equipped with a retroreflector and launched into an orbit of extended range. On the basis of our operating experience

* Regulations of the Federal Aviation Administration severely limited the possibilities for daylight ranging at Agassiz Station, but experience at McDonald Observatory has shown that the noise from the illuminated moon dominates that from the sky background whenever the sun's altitude is less than that of the moon.

and of recent technical advances, however, we recommend that the following improvements be made before the system is installed elsewhere. These improvements would increase the accuracy of the data, increase the system's repetition rate, and reduce the operational costs.

Probably the most important consideration for the laser is the pulse duration. Although the error of multielectron return pulses can be reduced to a value less than the pulse's half-width, greater accuracy is obtained more efficiently with shorter pulses. According to the manufacturer, the present laser could be rebuilt to have a pulse duration of 2 to 3 ns with a single-pulse energy of 30 J. This improvement would be made by using an internal or external shutter to advance the trailing edge of the oscillator pulse. A third amplifier would restore the energy lost by this reduction of the pulse duration. In a redesign of the oscillator, the single-transverse mode would be achieved without use of the pinhole, which has made oscillator alignment a rather critical procedure. The occasionally unstable flashtube sequence, which starts with the final amplifier and ends with the oscillator, can also be eliminated; it is possible to trigger all flashtubes simultaneously. With improved cooling, an increased pulse-repetition frequency of 1 min^{-1} appears to be possible. The use of a dichroic mirror with a flatter rear surface would improve the quality of the infrared beam, with consequent simplification of the alignment of the link between the transmitter and the receiver.

We recommend that, when possible, new observing sites be chosen for clear weather, low latitude, and low overhead air traffic. We also recommend that the pier that supports the transmitting unit be made large enough to allow the laser and coude telescope to be installed in separate rooms. With one additional prism, the laser beam could still be directed to the entrance window at the base of the telescope. The advantage of this arrangement is that the laser and its entire circulatory cooling system could be indoors, making it easier to keep the critical components at a constant temperature. It was difficult to maintain a constant temperature at Agassiz Station, where the ambient temperature variations at times were very large. If a television monitor were used for guiding, the observer could be indoors at a console, where he could also operate the laser — a task that currently requires a second person.

In addition to these changes, we also recommend that the optical elements of the telescope's coudé and divergence systems be modified for longer life at greater laser energy by using improved optical materials or by redesigning for lower energy densities.

Consideration should be given to more efficient methods of handling the input and output data, particularly if the laser's pulse-repetition rate is increased. It would be helpful to have a small computer at the site to obtain predicted ranges and lunar offsets and to enter data automatically into the range-gate generator and possibly into the transmitter's and receiver's offset stages. The 1- μ s precision of the range gate should also be improved to be consistent with the current accuracy of the range predictions. To eliminate the possibility of human error and to increase the efficiency of the data handling, the range-counter readings should be automatically printed out or punched on cards or tape. If the laser is modified for shorter pulse duration, a new, more accurate method of range calibration should be used.

1.4 Discussion

This section will attempt to put the results of the completed investigation into perspective. The task is difficult because neither laser technology nor systems requirements remain static. First there will be some general comments on the advantages and disadvantages of the extended-range system. Then this system, in its present configuration and also in a configuration for satellite ranging, will be compared with two ruby-laser systems: the Smithsonian Astrophysical Observatory (SAO) satellite-ranging system and the lunar-ranging system at McDonald Observatory.

The transmitter of the extended-range system is transportable. It can be used at established observing sites without greatly affecting the use of the 1.5-m instrument on which its photometric receiving package is mounted. Since the large telescope is used as a receiver only, there is no danger that the laser beam will damage its optics. In many cases, the drive errors of an older instrument are tolerable, which would not be the case if the telescope were also used to transmit the laser beam. The laser photometer is particularly sensitive and, when not being used for laser ranging, should prove valuable to the observatory for other astronomical observations. It includes a movable mirror, reticles, and eyepieces useful in alignment and offset guiding.

It is also interesting to note that the laser's output energy at its fundamental wavelength of $1.06\text{ }\mu\text{m}$ is 3.5 times greater than it is at the second harmonic, where it is now used. There is always the potential for a still more powerful system if more sensitive detectors at a wavelength of $1.06\text{ }\mu\text{m}$ were to be developed.

The physical separation of the transmitting and the receiving units could also be used to compensate for the fixed velocity aberration of a return from a retroreflector on a geostationary satellite.

The previous section showed that the pulse duration of the neodymium-glass laser could be decreased. It would be more difficult to decrease its 0.9-nm bandwidth to a value less than 0.1 nm , which can be obtained with a ruby laser. Hence, the bandwidth of the receiver's optical filter must be larger than that for a ruby laser. Consequently, the background noise will be somewhat higher, but not high enough to dominate the laser returns, which tend to be higher than those obtained with ruby-laser systems. This statement is evidenced by the fact that lunar returns were actually obtained after sunrise at one time and from the full moon at another.

When ranging to artificial satellites too distant for visual tracking, the transmitting mount must be positioned precisely in angle. This positioning could be accomplished by using the mount's stepping motors, which move the telescope at a low rate. However, if the telescope is to be slewed both rapidly and accurately from one pointing position to another, the drive system must be modified.

For a comparison with other laser systems, another configuration of the system (a satellite configuration) is considered. Its characteristics and those of the present configuration are given in the first two columns of Table 1. In the satellite configuration, the guide telescope is used to receive the laser return; the transmitting and the receiving units of the system are thus no longer separated. The transmitted beam-width is set at $100\text{ }\mu\text{rad}$ (21 arcsec) to compensate for the prediction and setting errors associated with the tracking of artificial satellites. The characteristics of SAO's ruby-laser system are given in the third column. It is assumed that the beam divergence of this system is set to its minimum value (120 arcsec). The characteristics of the lunar-ranging system at McDonald Observatory are given in the last column.

Table 1. Comparative characteristics of laser systems.

Characteristic of system	SAO extended-range laser system in present configuration	SAO extended-range laser system in satellite configuration	SAO ruby-laser system	McDonald ruby-laser system
η_T , optical efficiency of the transmitting telescope (%)	90	90	90	35
E, laser energy (J)	20	20	7.2	3
D_R , aperture diameter of receiving telescope (m)	1.55	0.2	0.51	2.72
θ_T , transmitted beamwidth (arcsec)	3.7	21	120	2
T, one-way atmospheric transmittance (%)	0.50	0.50	0.59	0.59
η_R , conversion efficiency of receiver (%)	6	6	1.7	0.6
λ , wavelength of laser radiation (nm)	530	530	694	694

Values of A_S/Ω_S are given in Table 2 for a number of retroreflectors. This ratio of effective area to solid angle is the quantity that characterizes a reflector in the range equation. For spherical satellites with metallic surfaces, A_S/Ω_S is $1/6 \text{ m}^2 \text{ sr}^{-1}$ for a diffuse sphere 1 m in diameter and $1/16 \text{ m}^2 \text{ sr}^{-1}$ for a specular sphere of the same size. For Pageos, which is 34.5 m in diameter, $A_S/\Omega_S = 74.4 \text{ m}^2 \text{ sr}^{-1}$ if specular reflection is assumed. The ranges of various artificial satellites at an altitude of 30° are given in Table 3. The value of 384 Mm is assumed for the moon.

Table 2. Optical characteristics of retroreflectors.

Retroreflector	$A_S/\Omega_S \text{ (m}^2 \text{ sr}^{-1}\text{)}$
Timation III	2.5×10^6
BE-B, BE-C	2.9×10^6
Lageos	6.2×10^6
Geos 1, Geos 2	1.3×10^7
Apollo 11, Apollo 14	4×10^7
Apollo 15	1.2×10^8

Table 3. Satellite ranges (artificial satellites at apogee, altitude 30°).

Satellite	Range (Mm)
BE-C	2.2
Geos 1	3.5
Lageos	5.2
Pageos	7.4
Timation III	16.4
Geostationary satellite	38.7
Moon	384

The performance characteristics of the systems of Table 1 were determined from the range equation and are plotted in Figures 1 to 4. It must be remembered in comparing these figures that the results are dependent on certain assumptions that may not be completely realized in practice. For example, the transmitted beam divergence of the currently configured extended-range system is taken to be 3.7 arcsec, but the return signal strength changes by 8 photoelectrons for each 1-arcsec difference

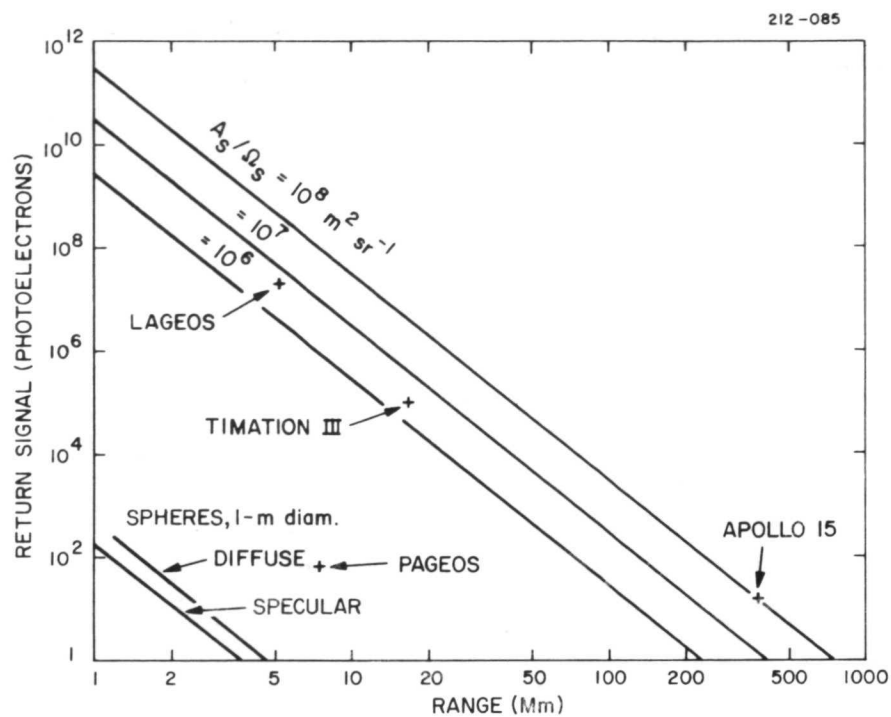


Figure 1. SAO extended-range laser in its present configuration.

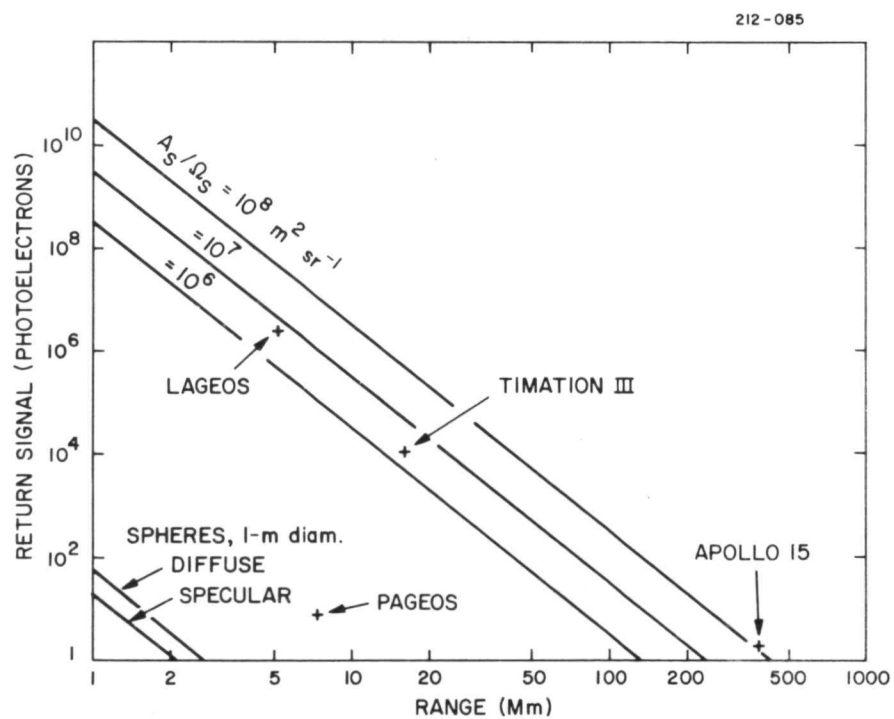


Figure 2. McDonald ruby-laser system.

from this value. The calculated return that this system receives from the Apollo 15 retroreflector is 15 photoelectrons for an altitude of 30° and an earth-moon distance of 384 Mm. The actual distance, however, varies between 350 and 400 Mm, with corresponding return-signal strengths from 17 to 10 photoelectrons. If the moon is overhead, the two-way transmission through the clear atmosphere is twice the value for an altitude of 30° . Hence, at low latitudes, returns from the Apollo 15 retroreflector would be anywhere between 10 and 34 photoelectrons when the full width of the transmitted laser beam is exactly 3.7 arcsec.

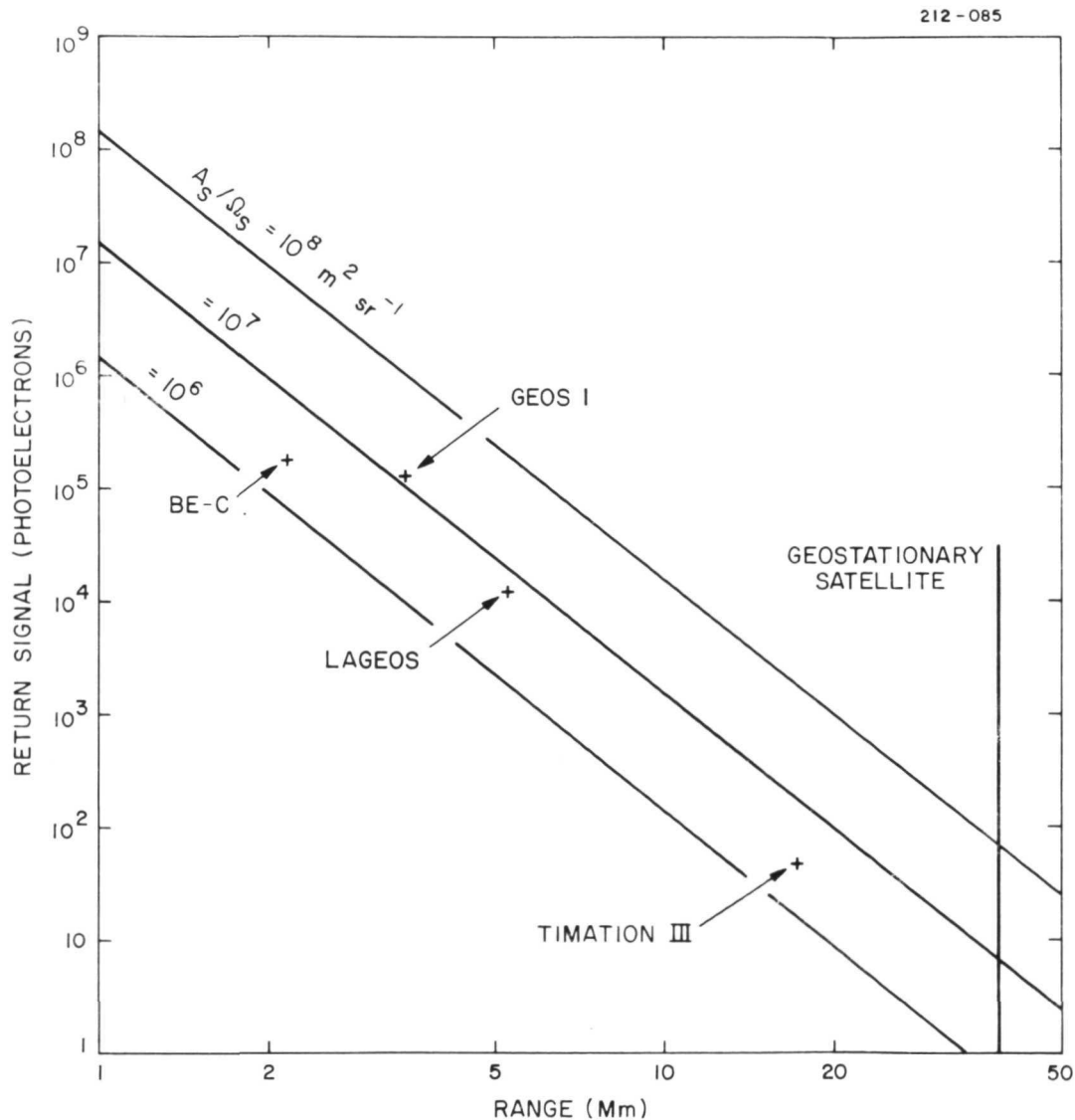


Figure 3. SAO extended-range laser in satellite configuration.

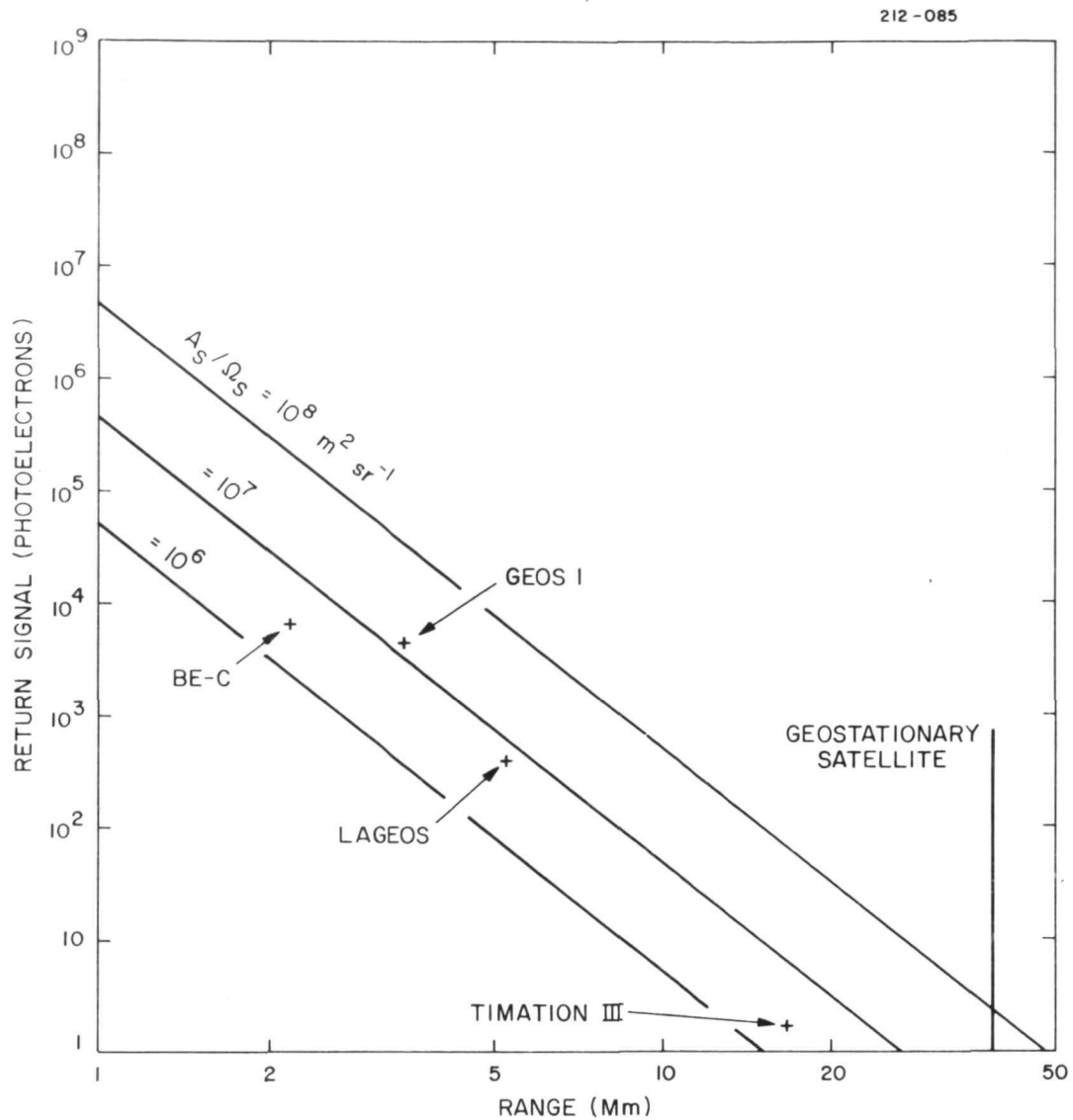


Figure 4. SAO ruby-laser system.

The comparison of the extended-range system with ruby-laser systems can be summarized by noting that in its current configuration, the calculated return from Apollo 15 is 15 photoelectrons, whereas the calculated value for the McDonald system is 2. The calculated return from Timation III is 50 electrons for the satellite configuration of the extended-range system and 2 for the SAO ruby-laser system when operated with minimum beamwidth.

2. DETAILS

2.1 Technical Background

The first laser pulse was transmitted to and returned from the lunar surface in 1962. Smullin and Fiocco (1962) used a 50-J ruby-laser oscillator built by Raytheon Company. Their experiment was performed only 2 years after the laser was invented, before Q-switching was in use and before the first retroreflector had been placed on the surface of the moon. Their accuracy was only 0.5 ms. That same year, a group at Princeton University suggested that a retroreflector be placed on the moon to enhance the reflected signal and to localize the point of reflection on the lunar surface. A Lunar-Ranging Experiment (LURE) group was formed and a system for precise ranging with a ruby laser proposed (Alley et al., 1965). In 1969, soon after the astronauts had placed the first retroreflector on the moon, the LURE group obtained their first return by using the 3-m telescope at the Lick Observatory in California (Faller and Wampler, 1970). The group then constructed a lunar laser system that uses the 2.7-m reflector at McDonald Observatory for regular observations (Silverberg and Currie, 1972). A second lunar laser system was built by the Air Force Cambridge Research Laboratory (AFCRL) (Carter et al., 1972). Other systems also using ruby lasers and large telescopes have been constructed in France (Orszag and Calamme, 1971), Japan (Tachibana et al., 1972), and the Soviet Union (Kokurin et al., 1972). The LURE group is currently building its second laser system, in Hawaii (Alley, 1971), which, like that described here, will use the second harmonic of the coherent radiation from neodymium ions, but it will use YAG rather than glass as the host material.

2.2 Chronology of the Program and Associated Events

1969

January 21	First visit to the Central Research Laboratory of the American Optical Corporation, Southbridge, Massachusetts, to discuss the use of the high-radiance laser for lunar ranging.
March	Proposal by SAO to NASA for \$429,815.

July 20	Placing of the first retroreflector on the surface of the moon, by the Apollo 11 astronauts.
October 23	First meeting with the FAA on the use of a high-powered laser at Agassiz Station.
November 1	Receipt by SAO of contract for \$100,000 from NASA.

1970

January 30	Start of the design of the temporary optics for close-satellite ranging.
February	Proposal by SAO to NASA for \$90,000.
March 4	Receipt by SAO of contract for \$99,830 from NASA.
April	Proposal by SAO to NASA for \$250,000.
June 15	Delivery of high-radiance laser to Agassiz Station.
July 6	Receipt by SAO of contract for \$89,272 from NASA.
November 6	Close-satellite ranging system in operation.
November 17	Landing of Lunakhod-I on the moon.

1971

February 9	Apollo 14 landing on the moon. Decision made to dismantle the close-satellite ranging system.
March 26	Installation of extended-range transmitting telescope at Agassiz Station.
August 7	Apollo 15 landing.
September 1	Receipt by SAO of contract for \$80,000 from NASA.
September 15	Installation of photometric package on the 1.5-m telescope at Agassiz Station.

1972

February 6	Start of lunar ranging.
May 23	First lunar return.
September 23	Series of six lunar returns in one night.
November 3	Fitting of SAO lunar returns of September 23 to an ephemeris by Dr. Derral Mulholland of the University of Texas at Austin.

2.3 Calculations of System Performance and Comparisons with Other Systems

The characteristics of the extended-range laser system are given in Table 4, and Table 5 compares it with other lunar-ranging systems. Figure 5 presents the range

equation and shows that the calculated value of the mean signal strength is 15 photoelectrons. Figure 6 shows a probability curve for returns of various strengths when the mean value of the Bose-Einstein (or geometric) probability distribution* is 15. There is a 94% probability of a return of 2 electrons or more, a 72% probability of 6 electrons, and a 40% probability that the signal will be equal to or greater than the mean value of 15 electrons.

Table 4. Characteristics of the extended-range laser system.

<u>Laser</u>	
Wavelength	530 nm
Spectral width	0.9 nm
Energy	20 J
Efficiency	0.035%
Pulse duration	25 ns
Beam diameter	20 mm
Beam divergence	37 arcsec
Repetition interval	5 min
<u>Transmitter</u>	
Aperture diameter	0.2 m
Optical efficiency	90%
Divergence of transmitted beam	3.7 arcsec
<u>Atmospheric Extinction</u>	
(one-way, at 30° altitude)	0.5
<u>Receiver</u>	
Aperture diameter	1.5 m
Quantum efficiency of photomultiplier tube	22
Conversion efficiency (electrons photon ⁻¹)	4 to 7%
Filter	
Spectral width	1.2 nm
Spatial width	10 arcsec
Background noise (average interval between electrons)	
Full moon	0.2 μs
Dark moon	10 μs
Return from Apollo 15 (calculated number of electrons given by range equation)	15

* See Goodman (1965) for an analysis showing that such a distribution should be used for a distant reflector having a large number of cube corners.

Table 5. Comparison of various lunar laser systems.

System	Reference	Wavelength (nm)	Energy (J)	Pulse duration (ns)	Pulse- repetition rate (min ⁻¹)	Aperture diameter of transmitter (m)
AFCRL	Carter <u>et al.</u> (1972)	694	1	2	12	1.5
French	Orszag and Calamme (1971)	694	3	60	?	1.0
Japanese	Tachibana <u>et al.</u> (1972)	694	5 to 6	20	6	1.9
LURE (McDonald)	Silverberg and Currie (1972)	694	3	3	20	2.7
LURE (Hawaii)	Alley (1971)	530	1	0.2	60	0.5
Russian	Kokurin <u>et al.</u> (1972)	694	4	21	4	2.5
SAO		530	20	25	0.2	0.2

$$N = \frac{\eta_T E}{2} \cdot \frac{A_R}{\Omega_T} \cdot \frac{A_S}{\Omega_S} \cdot \frac{1}{R^4} \cdot T^2 \cdot \eta_R \cdot \frac{1}{h\nu}$$

η_T , optical efficiency of the transmitting telescope	90%
E, laser energy	20 J
A_R , aperture area of the transmitting telescope	1.89 m^2
Ω_T , solid angle of the transmitted laser beam	$2.96 \times 10^{-10} \text{ sr}$
A_S/Ω_S , where A_S is the effective area and Ω_S is the solid angle of the beam returned from the Apollo 15 retroreflector	$1.2 \times 10^8 \text{ m}^2 \text{ sr}^{-1}$
R, distance to the moon	384 Mm
T, one-way atmospheric transmittance at 530 nm	50%
η_R , conversion efficiency (photoelectrons photon ⁻¹) of the receiver	6%
$h\nu$, energy of one photon at 530 nm	$3.75 \times 10^{-19} \text{ J}$
$\eta_T E/2$, energy transmitted within Ω_T	9.0 J
$N/\eta_T E$, gain of system	0.74 photoelectron J ⁻¹
N, strength of return	15 photoelectrons

Figure 5. The range equation for the extended-range laser system.

The diameter of the transmitted laser beam when it reaches the moon is 5.8 km, and that of the reflected beam returned to the ground, 6.7 km. The average return from the surface of the moon would be 0.3 photoelectron if no retroreflector were present.

2.4 The Laser

The laser is shown with the insulating cover removed in Figure 7 and in diagram form in Figure 8. The laser oscillator produces a 0.25-J, 1.06- μm pulse in a

single-transverse mode. The beam diameter is 3 mm. The oscillator's neodymium rod is 0.6 cm in diameter and 30 cm long, and the rod has a 5° bevel on each end. Three 64-cm-long flashtubes are close-coupled to the laser rod and pulsed with an energy of 1 kJ at a voltage of 2.8 kV. The right-hand mirror is a Brewster prism with a reflection of 4%. The left-hand mirror is a 99%, concave, dichroic reflector that focuses the beam on a diamond pinhole 28 μm in diameter. On the right-hand side of the pinhole, the beam is collimated with a lens and passed through the Pockels cell (KDP) and the calcite Glan-prism polarizer, which together comprise the Q-switch.

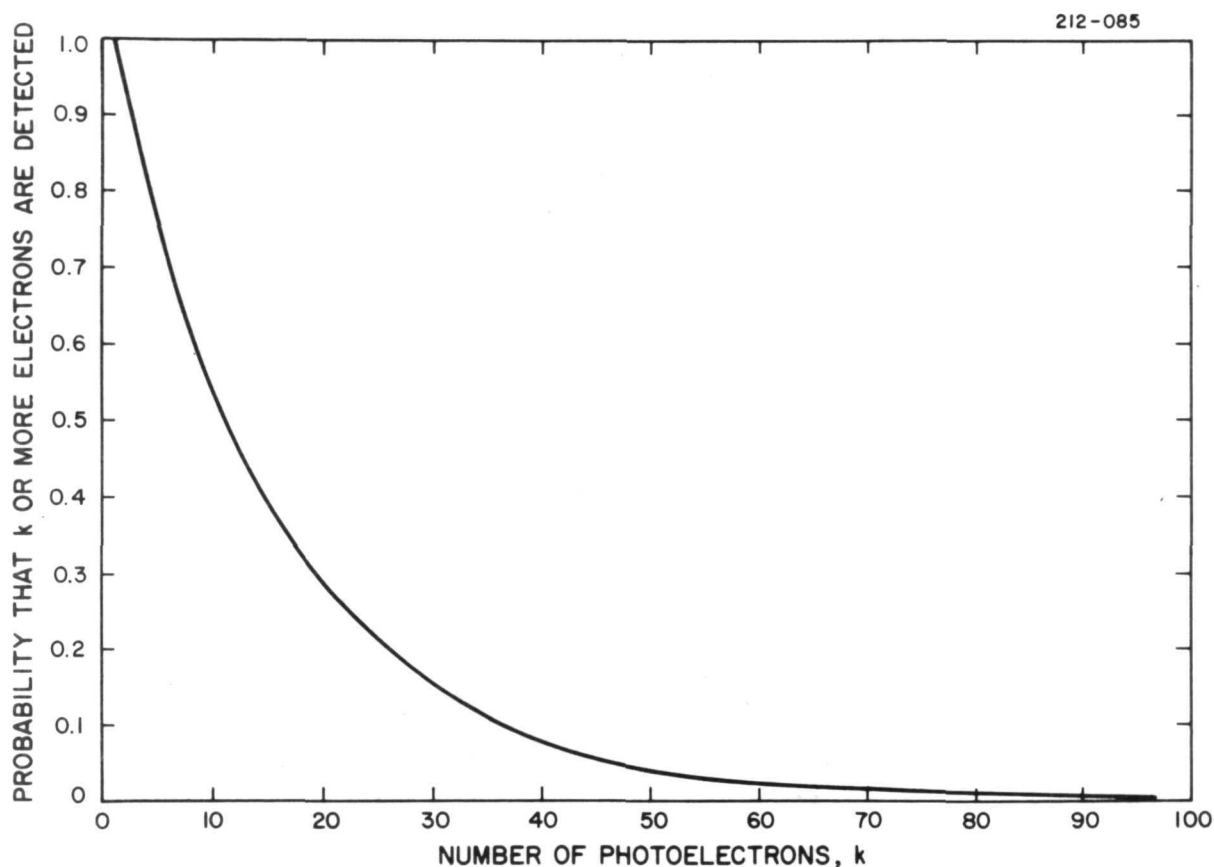


Figure 6. Probability that k or more electrons are detected when the average signal strength is 15 electrons.

After leaving the oscillator, the beam passes through the negative and positive lenses of a small Galilean telescope, which expands the diameter of the beam by a factor of 3. Then it is reflected by a mirror (gold on stainless steel) into the pre-amplifier. The preamplifier rod is 1.3 cm \times 54 cm. Each end is cut at Brewster's

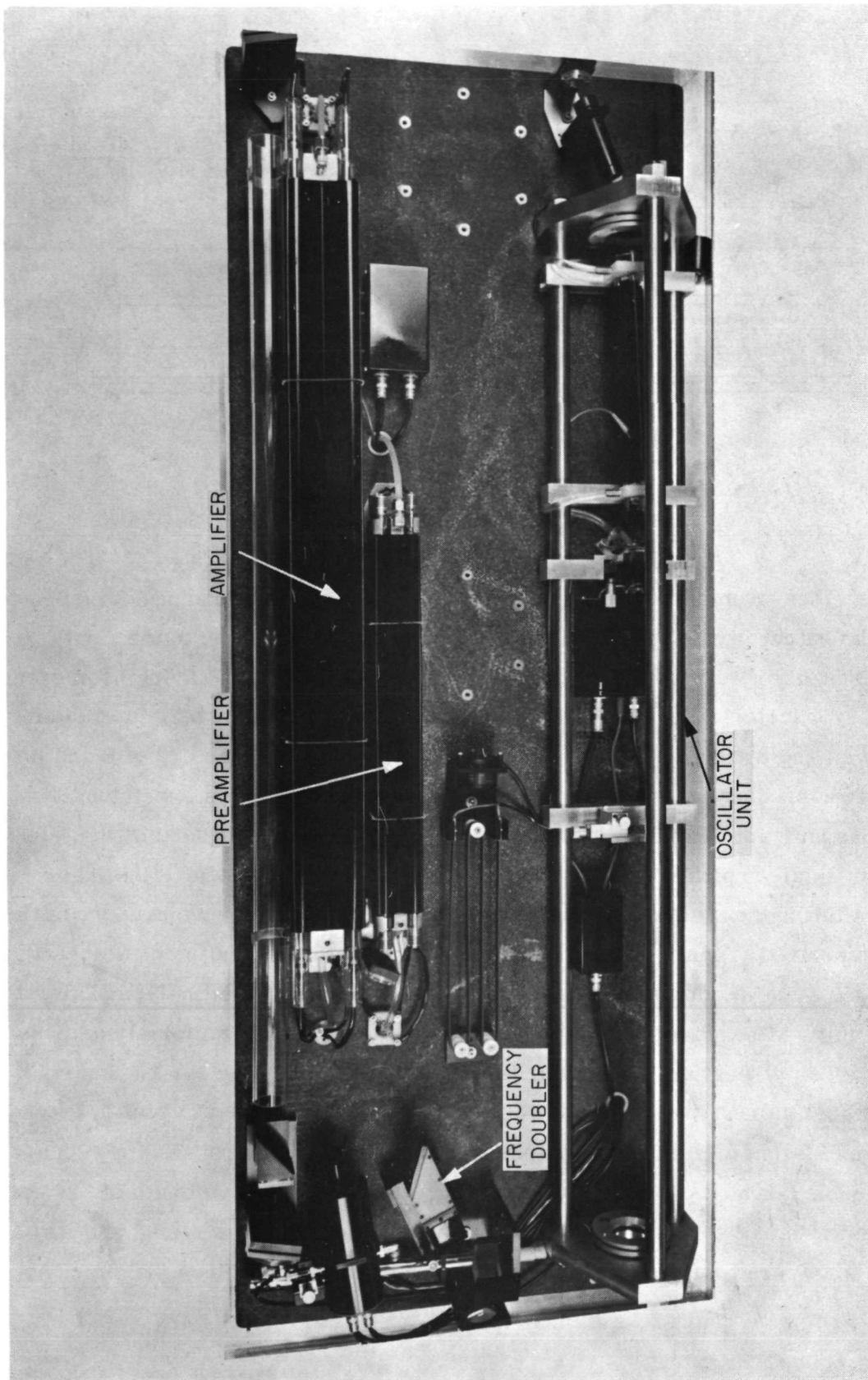


Figure 7. Photograph of the laser.

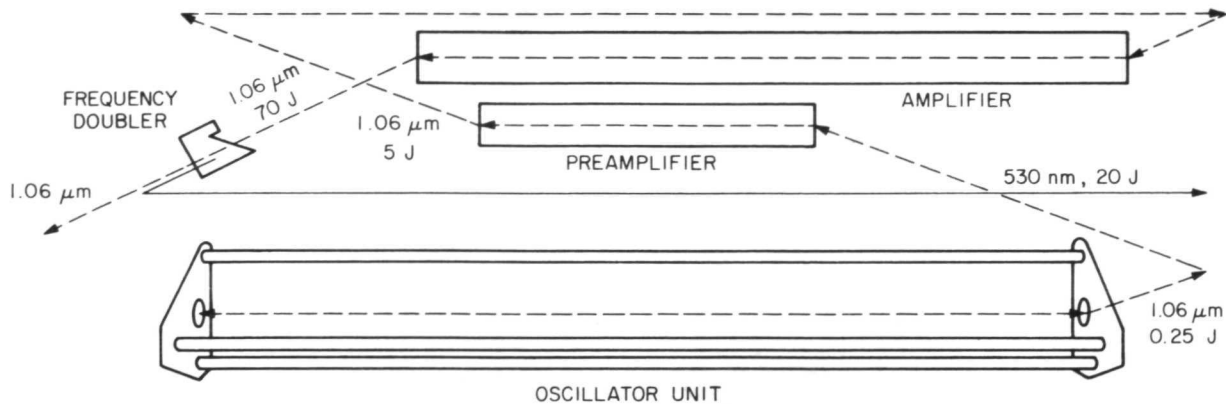


Figure 8. Diagram of the laser.

angle. Four close-coupled flashtubes, each 46 cm long, are pumped at 6 kJ (about 4.3 kV). The output is a 5-J, diffraction-limited beam that goes on to the final amplifier through a negative lens, a mirror, and a positive lens. Having been expanded in diameter by a factor of 5, the beam is passed through an aperture 3 cm in diameter, but on an angle, to give an elliptical cross section with diameters of 2 and 3 cm. This aperture increases the uniformity of the beam by removing its low-intensity outer portions and matching its cross section to the elliptical input face of the Brewster-cut final-amplifier rod. Before entering the final amplifier, the laser beam passes through a plastic tube, which reduces any air turbulence present in the insulated enclosure. Then a mirror directs the beam into the final amplifier, and the beam, now 3 cm in diameter, passes through the center of the final-amplifier rod (3.8 cm \times 1 m). Although this large rod is doped and pumped as uniformly as possible, the beam after amplification has a divergence twice the diffraction limit. Four 90-cm-long flash lamps, pumped with a total of 35 kJ at a voltage of about 4.3 kV, provide the excitation to produce an output of 70 J. This energy passes through a frequency doubler, which produces 20 J of energy at a central wavelength of 529.8 nm within a bandwidth of 0.9 nm. The diameter of this output beam is 2 cm, and its divergence is 180 μrad , which is about 4 times the diffraction limit at 530 nm. An

angular adjustment on the frequency doubler must be used when the temperature inside the insulated box is changed to preserve the phase matching between the fundamental and the second harmonic. A dichroic mirror reflects the 530-nm energy toward the base of the transmitting telescope. Some of the infrared energy (less than 3 J) is transmitted through the dichroic mirror and used for the link pulse. Some infrared energy is also reflected, but at a different angle from that of the visual energy. This reflected beam is blocked out before it enters the transmitting telescope.

The laser is powered by six capacitor units. Four of these units, 960 μf each, supply the four final-amplifier lamps; one unit (2 banks, 320 μf each) supplies the preamplifier, and one (within the control console) has three banks, 80 μf each, which supply the flash lamps of the oscillator.

A 10% aqueous solution of sodium nitrite is circulated around all three laser rods to absorb ultraviolet flashtube radiation that could otherwise solarize the rods. An electric heater and a fan hold the internal air temperature of the enclosed laser volume fixed. The temperature can be adjusted between 16° and 32°C and must always be higher than the nighttime ambient temperature. The higher range of temperature is used in summer, and the lower in winter when the ambient temperature may go down to -23°C. The laser's internal temperature must be decreased in winter because its heating system cannot support an inside-outside differential of more than about 40°C.

For mechanical stability, the laser is mounted on a granite block, which, in turn, rests on a concrete pier that is separate from the building.

The laser is pulsed in the following sequence: amplifier flash lamps, preamplifier flash lamps, oscillator flash lamps, Q-switch. A 1-mW, helium-neon, CW laser, mounted within the laser box, is used for preliminary alignment of the pulsed laser. Its 633-nm beam is adjusted to be coincident with the 530-nm beam.

2.5 The Transmitter

The extended-range transmitting (ERT) unit (shown photographically in Figures 9 and 10 and diagrammatically in Figure 11) collimates and directs the laser beam toward one of the retroreflectors on the moon. The unit consists of a coudé transmitting telescope and a separate guiding telescope, both on an equatorial mounting

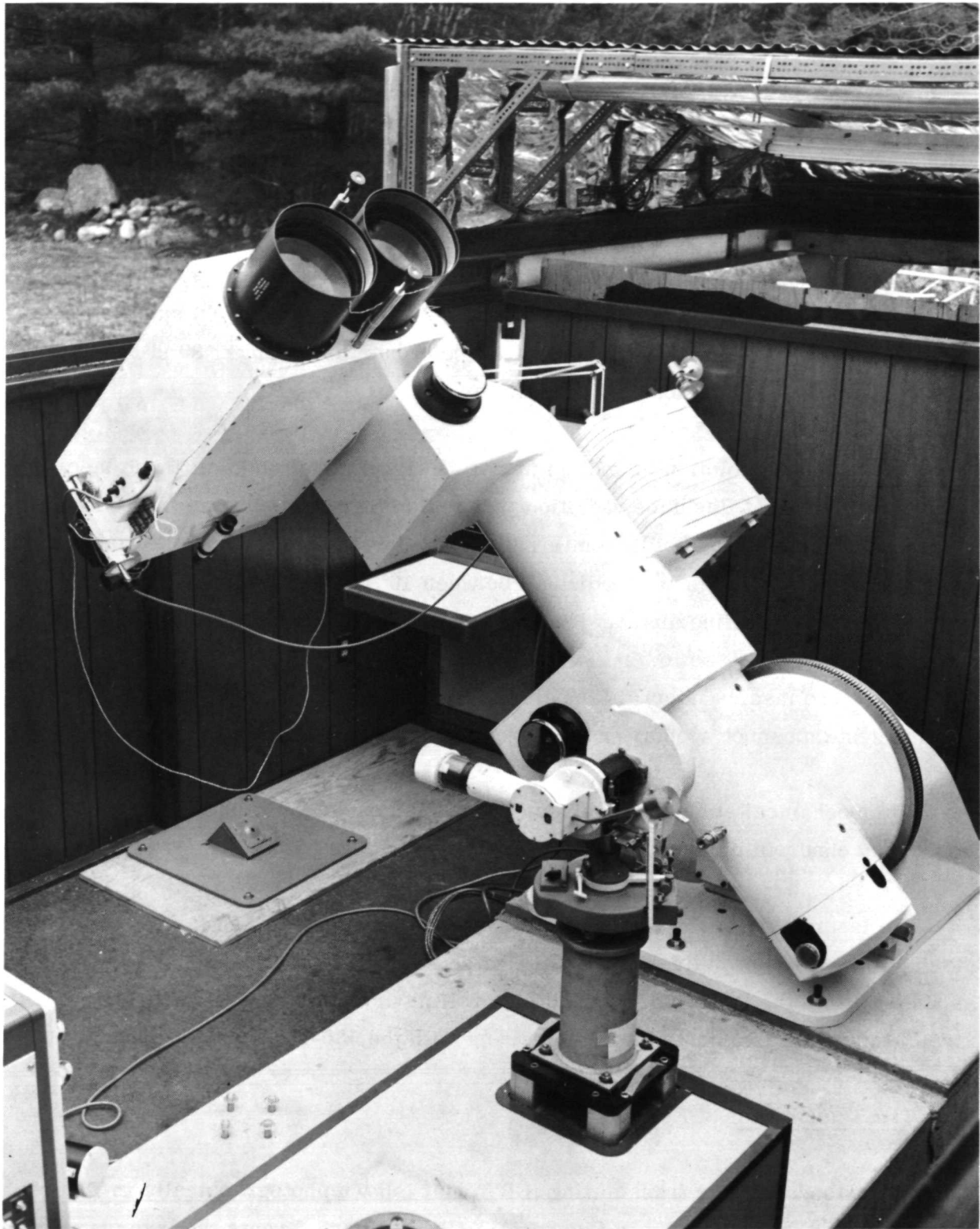


Figure 9. The transmitter.

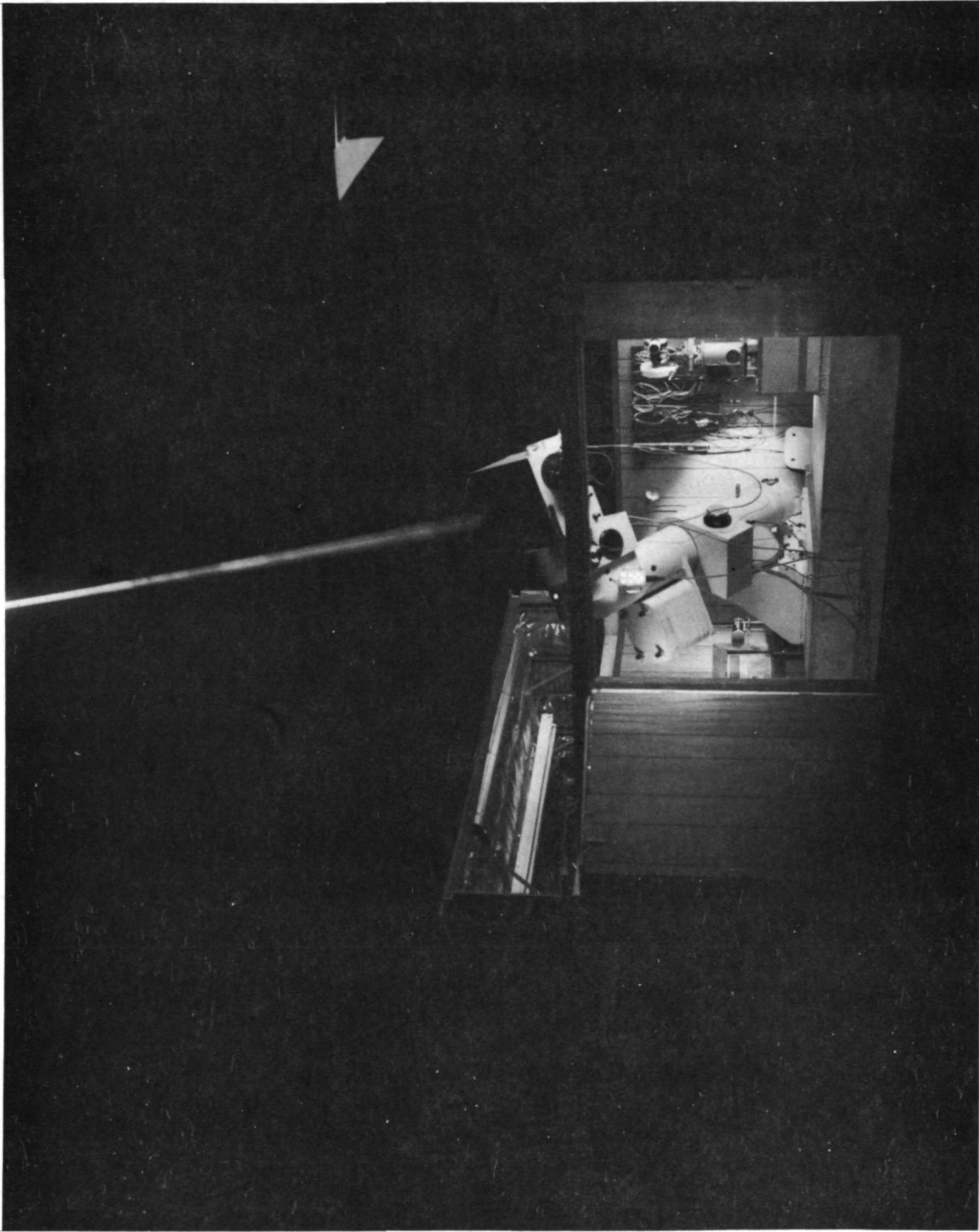


Figure 10. The transmitter at night, showing the laser beam.

pedestal that can be adjusted for any latitude. Prisms, rather than mirrors, are used as coudé elements in order to minimize damage from the high-intensity laser beam. They are made of crucible-grade crown glass with hard antireflection coatings. The optical system of the transmitting telescope provides for a continuous adjustment of the outgoing beam from 4 arcsec to 10 arcmin, with the lower setting used for lunar ranging. An offset mechanism permits a retroreflector in lunar darkness to be tracked by guiding on a visible feature at some other point on the surface of the moon. The characteristics of the transmitting unit are given below:

Drive:

Tracking:

R. A. rate: 0 to 15 arcsec s^{-1} eastward or westward

Dec. rate: 0 to 0.350 arcsec s^{-1} northward or southward

Guiding:

1-arcsec accuracy

Offsets up to 30 arcmin

Transmitting telescope (coudé refractor):

Aperture diameter 0.2 m

Focal length 1.0 m

Guiding telescope (achromatic refractor):

Aperture diameter 0.2 m

Focal length 1.4 m

Eyepieces:

24-mm focal length

16-mm focal length

3× Barlow lens

Measured plate scale: 3692 arcsec inch $^{-1}$

The manufacturer's calculated values of the beam spread as a function of the divergence setting are as follows:

Distance from zero-divergence position (inch)	Full beam spread (arcsec)
0.000	0.0
0.050	41.0
0.100	104.0
0.200	208.0

In the field, the divergence was set to minimize the angular diameter of the beam with the laser pulsed every 5 min. This setting was accomplished by placing the seven-hole Hartmann mask (shown in Figure 12) over the telescope's 0.2-m aperture and recording a Fresnel pattern (Figure 13) on photographic paper at a distance of 200 m. A quantity proportional to the divergence was obtained by measuring the 21 distances between the centers of the 7 spots and subtracting them from the corresponding values on the mask. This was done for 10 different divergence settings, and 21 curves of spot spacing versus divergence setting were plotted. Minimum values from each curve were averaged to give the minimum setting with a statistical error of 9.8 mils, equivalent to about 10 arcsec.

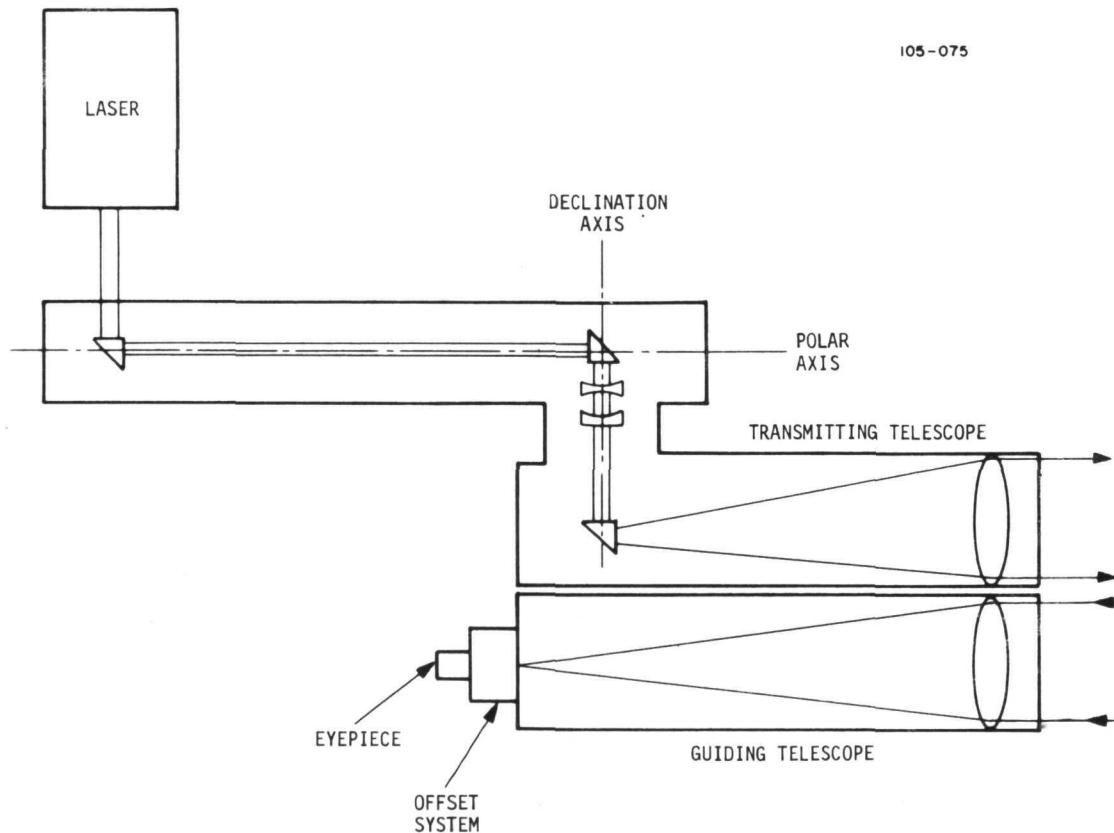


Figure 11. Optical diagram of the transmitter.

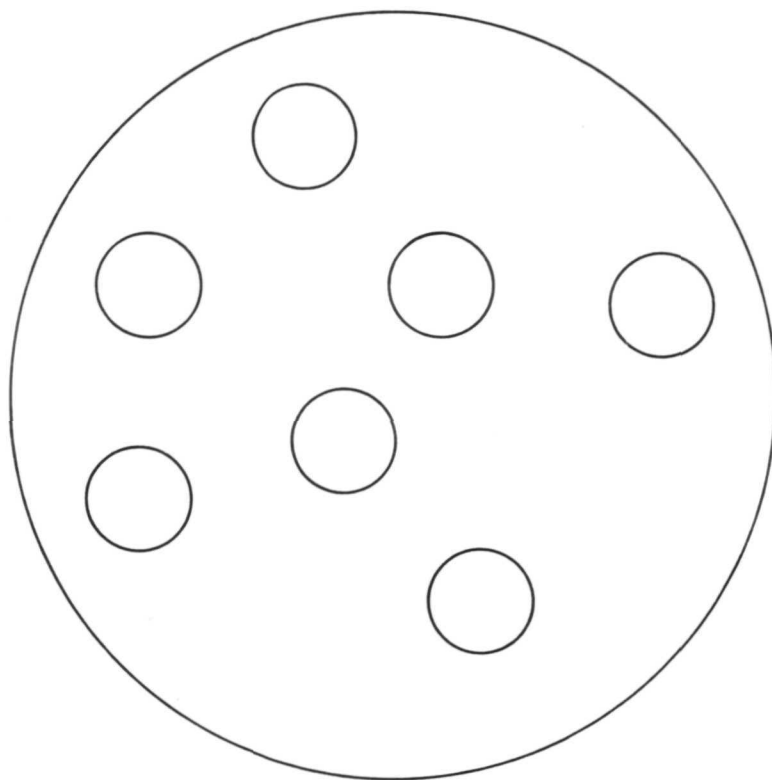


Figure 12. Hartmann mask used in setting the transmitted laser beam to minimum divergence.

Boresighting the coudé transmitting telescope and the guiding telescope was accomplished as follows. First, a helium-neon laser was aligned to make its beam coincident with and parallel to the system's pulsed green beam. The coudé prisms were adjusted so that the helium-neon beam left the transmitting telescope coincident with and parallel to the optical axis of the telescope for all pointing positions. A section of a 0.2-m retroreflector was placed across the objectives of the two telescopes. This retroreflector sampled the outgoing helium-neon beam and redirected it into the guide telescope. The cross hairs of the guide telescope were then set to the focused image of the helium-neon beam. To correct for dispersion between the green beam and the helium-neon beam, a piece of mylar was placed in the focal plane of the guide scope and the green beam was pulsed through the telescope and retroreflector. The pulse produced a small burn on the mylar at the focus of the green beam, and the

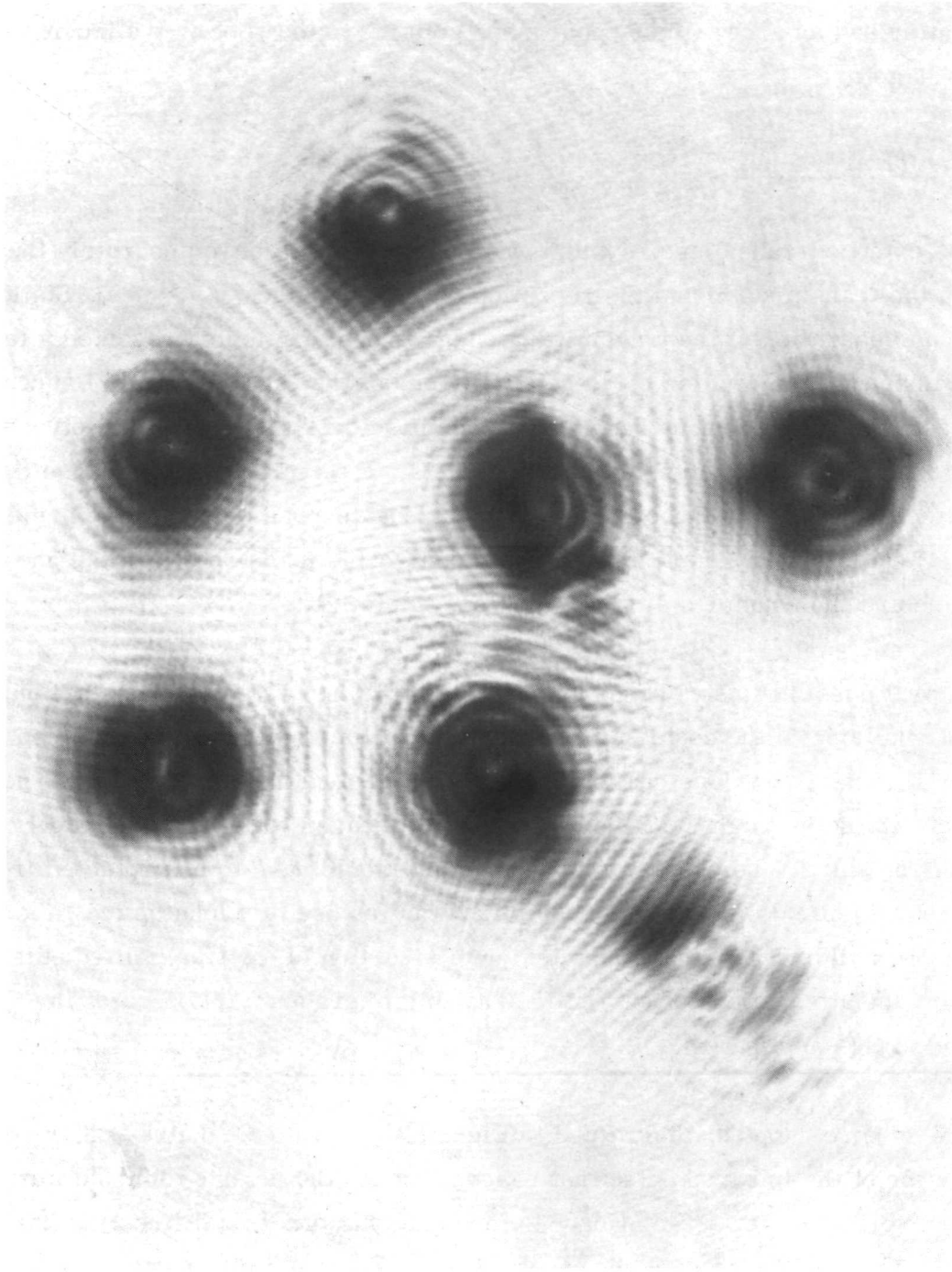


Figure 13. Fresnel pattern at 200 m from the Hartmann mask of Figure 12.

cross hairs were adjusted to the burn. As a final check and as a monitor of changes, the backscatter of the green beam was observed during ranging operations. This backscatter had an arrow-like appearance, pointing to the spot on the moon where the beam was going.

2.6 The Infrared Link

The extended-range laser system was designed to measure accurately the time between the transmission and the reception of a laser pulse. At Agassiz Station, the 237-m separation of the transmitting and the receiving units presented a technical problem because the counter could be at only one of the two locations. Hence, a pulse from the other location had to be transmitted over the distance involved without the introduction of a variable delay (a fixed delay is permissible). Because the received signal is close to the noise level, the counter was placed in the same building as the 1.5-m telescope; as a result, the coaxial-cable losses between the photomultiplier tube and the counter's stop circuit were minimized.

Several possibilities were considered for the transmission of the start pulse from the laser building to the counter. One was that the outgoing beam be sampled, detected, and sent through a low-loss coaxial cable. This method had disadvantages, however: 1) Electrical noise might be transmitted from the laser building to the receiving electronics, and 2) the cable was expensive and would have to be protected from moisture and animals. A second possibility was the use of a long optical fiber between the buildings for the transmission of a portion of the transmitted pulse. However, the attenuations of currently available fibers are far too great for the length required in this application.

The scheme adopted, diagramed in Figure 14, is an optical link that transmits that portion of the infrared pulse that passes through the laser's dichroic mirror and is not converted to visual radiation. Before entering the optical link, the infrared pulse is attenuated to the safe eye level. For added safety, the beam is transmitted at a height of about 3 m above ground.

The safe limit of laser radiation, depending on the standard used (Clarke, 1971), is between 9×10^{-5} and $1 \times 10^{-8} \text{ J cm}^{-2}$. According to Mr. David Sliney, Army

Surgeon General's Office, Edgewood Arsenal, Maryland, the upper limit appears to be more applicable to our situation, because the eye is less sensitive to radiation at $1.06 \mu\text{m}$ than it is to the more common, shorter wavelength laser radiation.

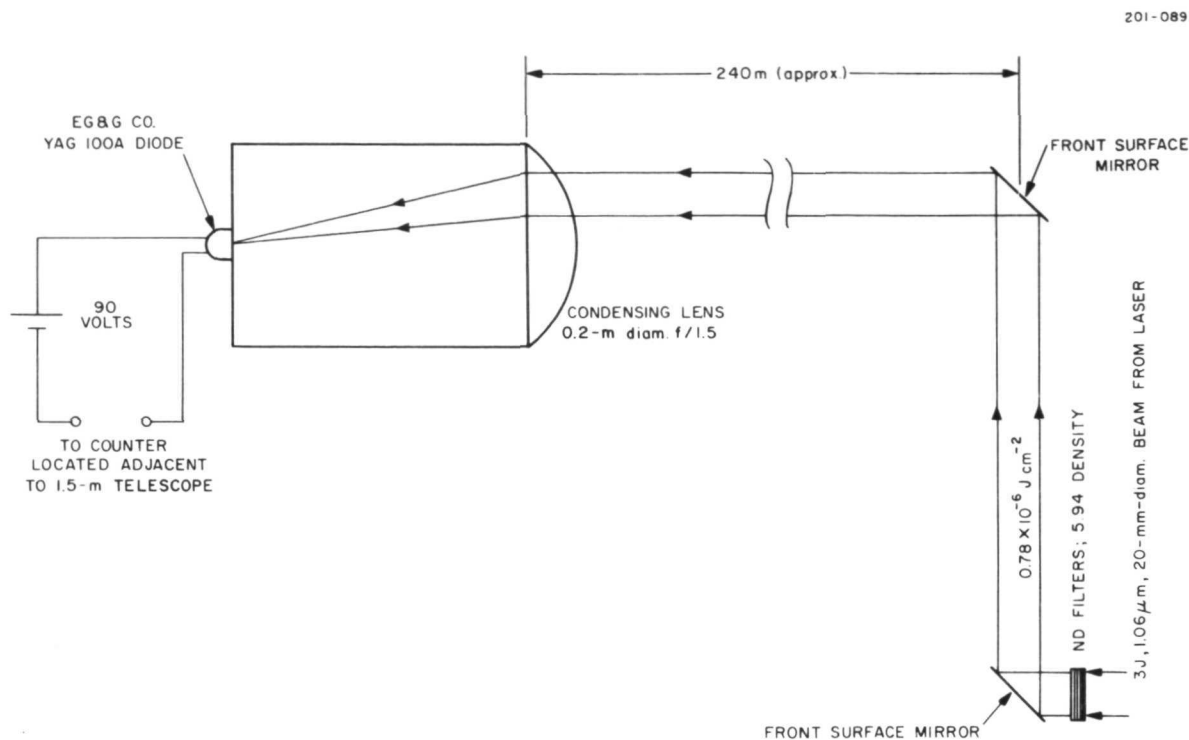


Figure 14. Diagram of the infrared link that connects the transmitting and the receiving telescopes.

Repeated measurements showed that the energy of the infrared pulse is always less than 3 J and its cross section is elliptical with axes 2.8 and 2.0 cm in diameter, an area of 4.4 cm^2 . Hence, the energy density is less than 0.68 J cm^{-2} before attenuation, and less than $0.78 \times 10^{-6} \text{ J cm}^{-2}$ after passing through a 5.94 neutral-density filter. Since the filter is inside the laser box, the radiation level is safe at all exposed positions. The 5.94 neutral-density filter is made up of two glass filters of 4.0 and 0.7 neutral density, each calibrated at $1.06 \mu\text{m}$, and four Kodak No. 96 Wratten filters with nominal values of 2.0, 0.3, 0.3, and 0.1 neutral density. The glass filters pass the infrared pulse without damage and reduce the intensity below the damage level of the Wratten filters. Since the density of a Wratten filter at $1.06 \mu\text{m}$ is 0.46 times its nominal value (Eastman Kodak, 1971), the effective density of the four filters in combination is 1.24.

The diameter of the infrared beam should be only about 7 cm after it has traveled the 237 m from the laser building. However, it is about 10 times that value and its cross-sectional intensity distribution is not uniform. The reason is that because this application was not in mind originally, the back side of the laser's dichroic mirror was not smoothly polished and the emitted infrared beam is therefore distorted.

The link is roughly aligned with a helium-neon laser whose beam had previously been adjusted for coincidence with the infrared beam. Then the neutral-density package is removed and the alignment completed by observing the small amount of visual radiation that accompanies the infrared beam and by burning a spot on a piece of exposed Polaroid film at the focus of the 0.2-m condensing lens. Of course, when the neutral-density filters are not used, the visual radiation can be safely observed only through special eyeglasses that block the infrared beam. When the filters are removed, a watch must be kept to be sure that the laser is not pulsed when anyone without such glasses is in a position where direct, reflected, or scattered light from the beam could enter his eye.

Once the rough alignment with the helium-neon laser has been completed, final adjustments can often be made without removing the neutral-density package. These adjustments are accomplished by using the mirrors at the laser building to steer the beam through small angles. The amplitude of the pulse detected at the far end of the link is observed on an oscilloscope. When the beam is pointed to maximize this amplitude, the link is aligned.

2.7 The Receiver

Figure 15 shows Harvard's 1.5-m telescope at Agassiz Station. The photomultiplier package of the laser system at this telescope's Newtonian focus is given in diagram form in Figure 16. Figure 17 shows how offset guiding is done by use of a diagonal mirror with a central hole. With the proper right ascension and declination offsets set in, a small crater or peak on the moon will appear on the eyepiece reticle when one of the retroreflectors on the moon is within the field of the photomultiplier. Offset guiding is used when the retroreflector is not sunlit or when its position cannot be readily identified from surrounding features. When sunlit, the Apollo 15 retroreflector, which is in mountainous terrain, can be tracked directly. In the direct-tracking mode, the hole in the mirror is closed with a mating piece (not shown in

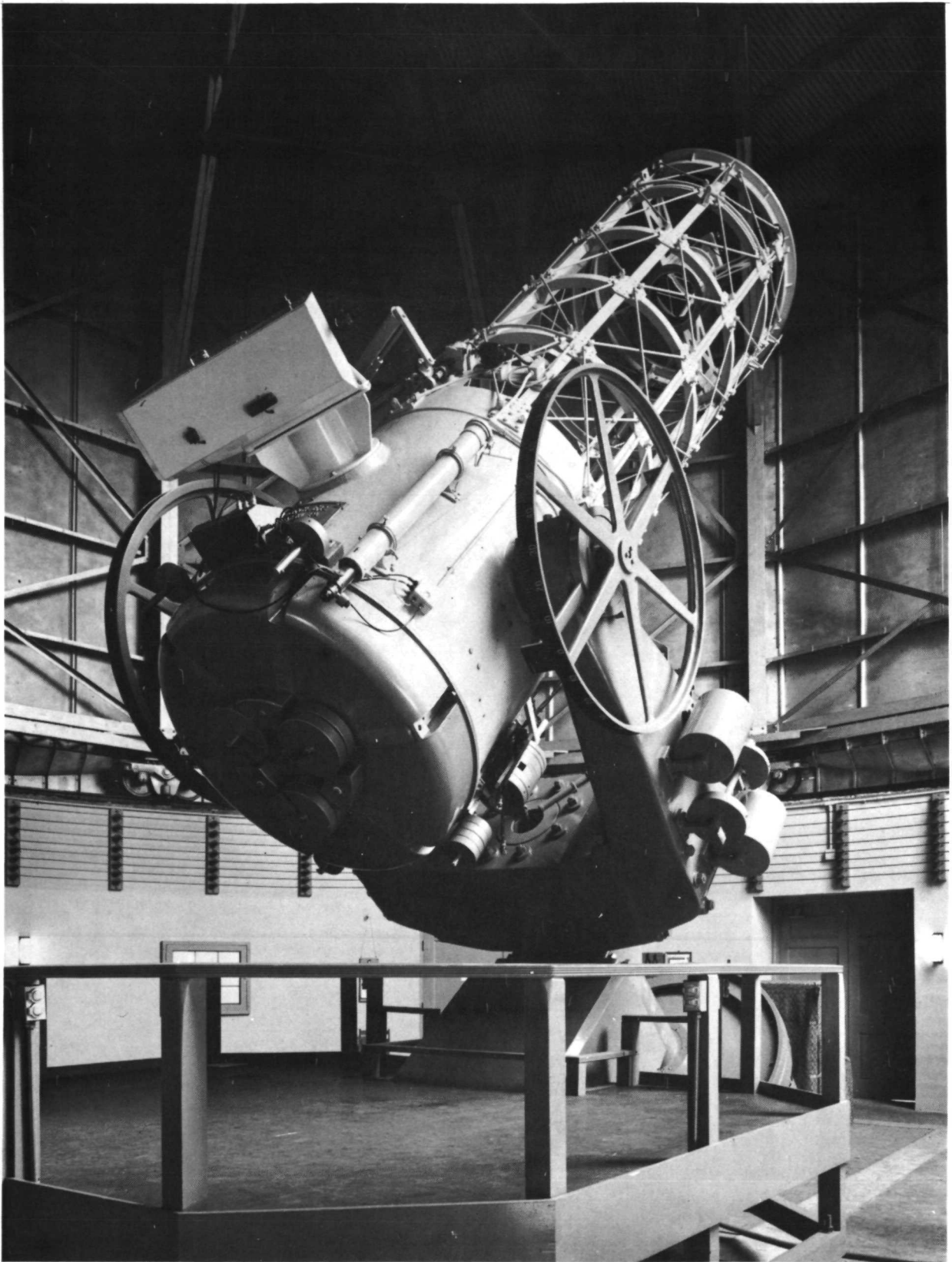


Figure 15. The 1.5-m telescope.

Figure 17), the offsets are reduced to zero, and the telescope is moved so that the reticle remains on the retroreflector. The mirror is opened shortly before the laser return is expected. The telescope keeps moving in hour angle at the lunar rate after the mirror has been opened. The declination remains fixed because the telescope has no declination-velocity drive. Even so, the retroreflector stays within the field of the photomultiplier tube when the field is not too small and the mirror is not left open too long.

105-075

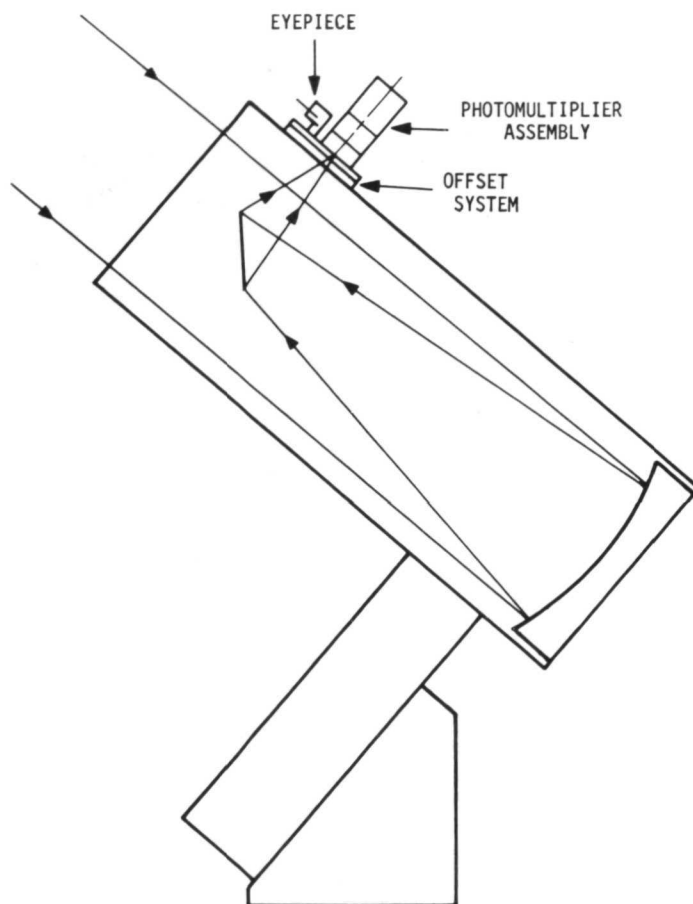


Figure 16. Optical diagram of the receiver.

The field stop can readily be set to any of the values given below:

Field-stop number	Field-stop diameter	
	(mm)	(arcsec)
1	0.152	4.0
2	0.228	6.0
3	0.404	10.5
4	0.940	24.6
5	1.600	42.0
6	3.20	82.0
7	9.00	180

Field stop 3 (10.5 arcsec) was the most commonly used.

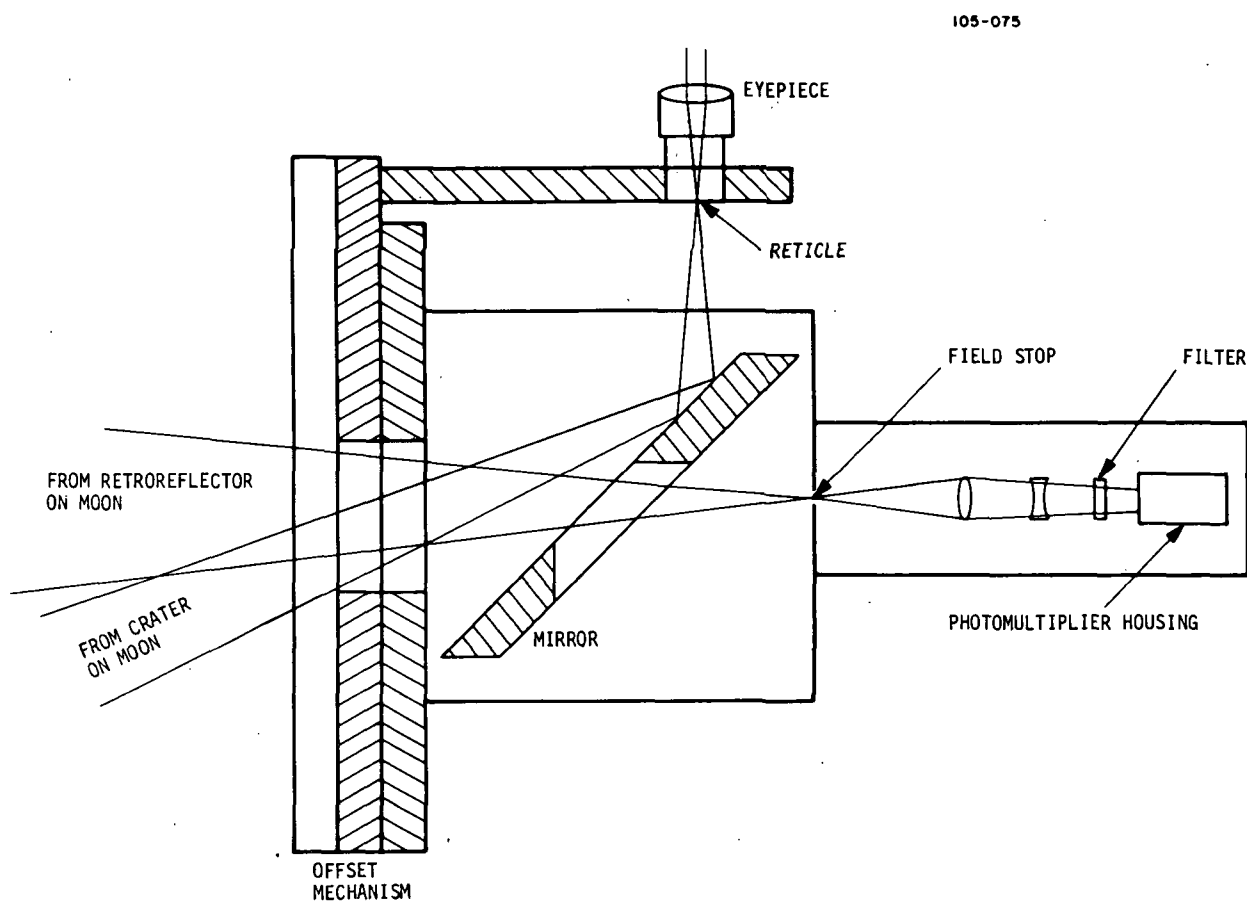


Figure 17. The offset system and the photomultiplier assembly.

The telescope's focal length at the Newtonian focus is 7.88 m; the corresponding plate scale is $26.2 \text{ arcsec mm}^{-1}$. Measurements made between the lunar peaks Pico and Piton confirmed this value.

The optical filter was made by Spectrum Systems Division, Barnes Engineering Co., Waltham, Massachusetts. Its central wavelength (measured at the factory) was 530.0 nm at 23°C, with a wavelength-temperature variation of +0.014 nm per °C. Thus, the central wavelength at the operating temperature of 0°C is 529.7 nm. The width of the filter between half-power points is 1.2 nm, and its transmission at the central wavelength is 52%.

According to the manufacturer, the wavelength of the laser is somewhere between 529 and 530 nm and its bandwidth between half-power points is 0.9 nm. Hence, there could be laser radiation above the half-power level anywhere in the interval 528.55 to 530.45 nm. Since the half-power limits of the filters are 529.1 and 530.3 nm, it is possible that, with the laser wavelength at its lowest value, the filter band would overlap only 39% of the laser band. A range calibration on September 23, 1972 (see Section 2.8), showed that this situation did not occur in practice. In the course of this calibration, the laser beam, greatly attenuated, entered the receiving telescope and was detected by the photomultiplier tube. The filter transmission was measured by observing the detected pulse amplitude with the filter in and out. The ratio of these amplitudes, which came out to be 45%, is the filter's transmission for the laser's radiation. Since the filter's transmission varies between 26 and 52% over its bandwidth, the measured value of 45% shows that the central wavelengths of the laser and of the filter were well matched.

The portion of the photometric package containing the filter and the photomultiplier tube was thermoelectrically cooled with the TE-102TS unit manufactured by Products for Research, Inc., Danvers, Massachusetts. The cooling served the dual purpose of reducing the tube's dark current and stabilizing the central wavelength of the interference filter. The latter function was the more important one when an illuminated retroreflector was tracked and the background rather than the dark current was the dominant cause of receiver noise.

Early in 1971, the decision was made to use the RCA C31034A photomultiplier tube, which had just come on the market. This tube uses a GaAs photocathode, instead of the usual alkali cathode, with the advantage of a higher quantum efficiency at 530 nm. The principal disadvantages are the small cathode size (4 mm \times 10 mm) and the low, 1 μ A maximum value of anode current. Neither disadvantage was particularly serious. The first C31034A tube exhibited noise pulses that occurred randomly at a rate somewhat less than 1 kHz, along with excessive and fluctuating dark current. It was replaced by a second tube, obtained after RCA had improved its processing. The second tube operated satisfactorily and was used until the close of the program. When measured at the factory on January 24, 1972, the tube's quantum efficiency at 530 nm was 23% and its gain was 2.1×10^6 at 1.8 kV. When measured there again on August 1, after being used in the system, the quantum efficiency was 20% and the gain was 1.1×10^6 . Our own gain measurements, made on April 7 and September 22, were 3.1×10^6 and 1.8×10^6 , respectively. The factory measurements were conducted by using a standard lamp and measuring anode current under the usual operating conditions, with the tube's amplifier section shorted out. Our measurements were performed by reading the tube's anode current and simultaneously using oscilloscope photographs to count the average number of photoelectrons generated in a given time interval. The single-electron distribution, shown in Figure 18, was also determined from these photographs. The value of the single-electron resolution, calculated from the width of this curve, was 52%.

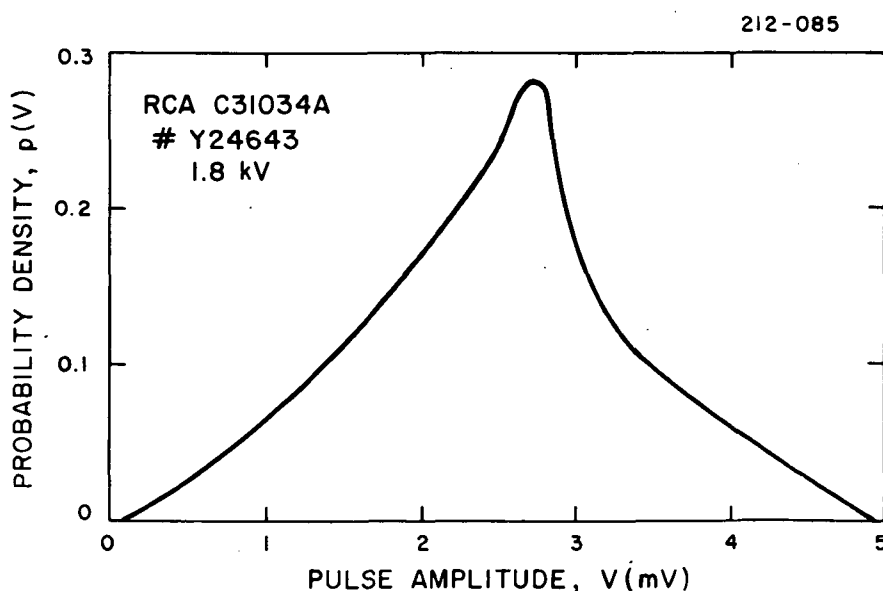


Figure 18. Single-electron distribution.

The receiving electronics are diagramed in Figure 19. The variable attenuator and the 30-dB and 76-dB amplifiers supplement the gain of the PMT and set the output signal voltage relative to the counter's fixed threshold.

The threshold setting is made for an optimum signal-to-noise discrimination. The 0-dB amplifier in the video chain stretches the duration of the single-photoelectron pulses from the PMT to a value larger than the laser pulse. This stretching removes the structure of the returned pulse, making the pulse amplitude roughly proportional to the number of photoelectrons in the return. In this way, the probability of detecting a multielectron return is increased, at the expense of the increased range accuracy that could be obtained from an analysis of the pulse's structure. The pulse stretcher, which follows the infrared detector, facilitates the start of the counters and the range-gate generator. The overall video gain is set so that return signals at the two-electron level and above stop the 0.1-ns counter. The 10-ns counter gives a precise measurement of the delay of the range-gate generator, which can be set only to the nearest microsecond. The "gate" and "window" pulses start at the end of the delay. The window pulse opens the STOP circuit of the 0.1-ns counter for 200 μ s; the gate pulse starts the sweep of oscilloscope A. The oscilloscopes display all the photoelectrons from the photomultiplier tube over the duration of their respective sweeps. Oscilloscope A, with its 5- μ s sweep, always displays the pulse that stops the 0.1-ns counter. It is used to confirm a return when its amplitude is above the single-electron noise level. With its 1- μ s sweep, oscilloscope B displays a majority of the returns but misses others because the start of the sweep is limited by the 1- μ s precision of the range-gate generator. When a single-electron return is displayed on oscilloscope B, its range can be determined from the photograph of the return. The accuracy, however, is less than that of the 0.1-ns counter, which stops on the multielectron returns. The transit times for the single-electron returns displayed on oscilloscope B are the sums of the time scaled from the oscilloscope trace, the delay set into oscilloscope A (which was accurately measured), and the reading of the 10-ns counter.

Additional information on some of the components of the receiving system is given on the following page.

<u>Item</u>	<u>Manufacturer and model number</u>
Pulse stretcher	Hewlett-Packard pulse generator, Model No. 222A
10-ns counter	El Dorado, Model No. 783-G
0.1-ns counter	Nanofast, Model No. 536B
Quartz oscillator used to drive both counters (not shown in Figure 19)	Hewlett-Packard, Model No. 105B
Range-gate generator	SAO, Model No. 3003
Oscilloscope A	Tektronix, Model No. 454A
Oscilloscope B	Tektronix, Model No. 7904
0- to 50-dB attenuator	Texscan, Model No. RA 54
30-dB amplifier	C-COR., Model No. 3310
0-dB, 20-MHz amplifier	Dynair Electronics video distribution amplifier, Model No. DA 234A
76-dB amplifier	C-COR., Model No. 1375-P

212-085

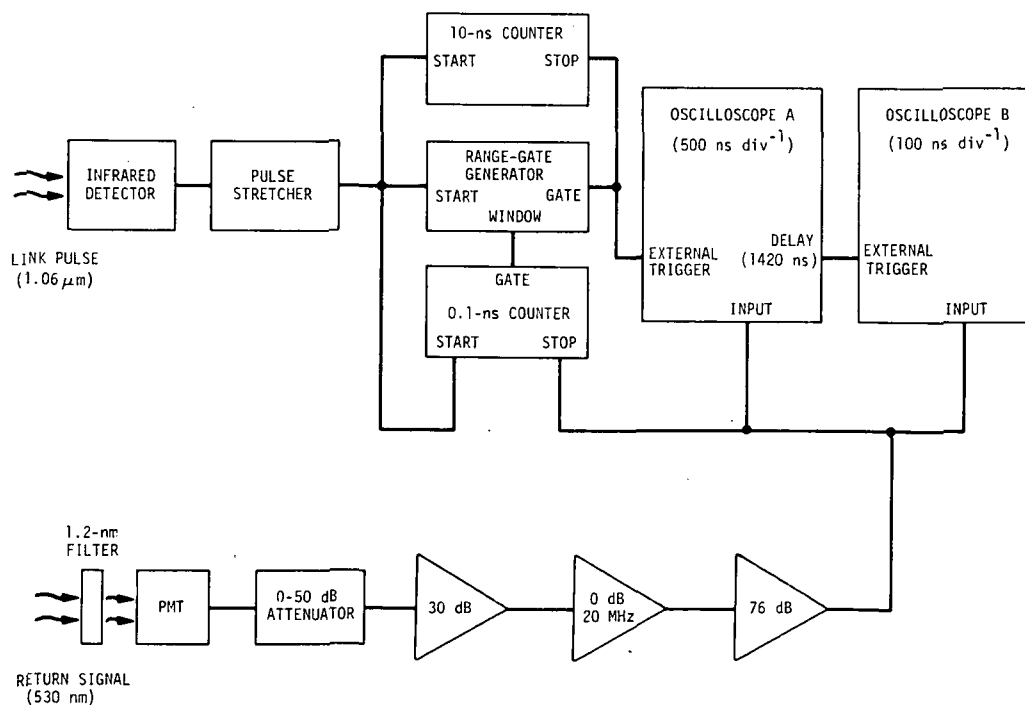


Figure 19. Block diagram of the receiving electronics.

If we assume that the reflectance of each mirror in the large telescope is 90%, the transmission of the interference filter is 50%, and the quantum efficiency of the photomultiplier is 20%, then the overall conversion efficiency (photoelectrons photon⁻¹) is 8%. This is an important quantity characterizing the sensitivity of the receiver. It was measured a number of times during the experiment by using bright stars, whose spectral flux densities are known, as photometric sources.

The conversion efficiency η is obtained by measuring the stellar light flux F (photons s⁻¹) that enters the telescope and determining the cathode current I (photoelectrons s⁻¹) at the cathode of the photomultiplier tube. The following relation is used:

$$\eta = \frac{I}{F} \text{ (electrons photon}^{-1}\text{)} \quad (1)$$

The quantity I is obtained by dividing the measured anode current of the PMT by the gain of the tube. The light flux F is determined from the tables of Mitchell and Johnson (1969). From their Table 2, we find that the absolute flux density of a zero-magnitude A0V star in filter band 52 (which includes the laser wavelength 530 nm) is $4.69 \times 10^{-12} \text{ W cm}^{-2} \mu\text{m}^{-1}$. To convert this value to the rate of photons entering the 1.5-m telescope, we multiply by

$$1.89 \times 10^4, \text{ the aperture area of the telescope, in cm}^2$$

and

$$1.2 \times 10^{-3}, \text{ the bandwidth of the interference filter, in } \mu\text{m}$$

and divide by

$$3.75 \times 10^{-19}, \text{ the energy of a photon at 530 nm, in J.}$$

The result is then modified by multiplying first by ℓ_S/ℓ_A , the ratio of the flux from the calibration star to that from the A0V star, and then by the atmospheric extinction T . The ratio ℓ_S/ℓ_A is obtained from

$$\log_{10} \frac{\ell_A}{\ell_S} = 0.4 x \quad (2)$$

where x is the value in column "52," Table 7, of Mitchell and Johnson, for the bright star being used for the measurement. The atmospheric extinction is obtained from (Kaula, 1962, p. 256)

$$T = \exp (-\tau \cos Z) , \quad (3)$$

where $\tau = 0.0090\lambda^{-4} + 0.223$, Z is the zenith distance of the star, and λ is the laser wavelength in μm . For a wavelength of 530 nm, we have

$$T = \exp (-0.337 \cos Z) . \quad (4)$$

The zenith distance comes from the relation (Sidgwick, 1971, p. 509)

$$\cos Z = \sin \delta \sin \phi + \cos \delta \cos \phi \cos (\alpha - \theta) , \quad (5)$$

where δ is the declination of the star, ϕ is the latitude of the telescope, α is the right ascension of the star, and θ is the sidereal time. By use of the latitude of Agassiz Station and the fact that the hour angle H is $\alpha - \theta$, equation (5) becomes

$$\cos Z = 0.673 \sin \delta + 0.739 \cos \delta \cos H . \quad (6)$$

We employed this method on December 12, 1971, to measure the receiver's conversion efficiency. The night was clear and a 5.5-mag star was visible to the naked eye. The stars α Peg and σ Cet were used, and the results gave $4\% < \eta < 7\%$. The conversion efficiency was measured again on April 17. The stars β Leo and θ Leo were utilized, and the values obtained again ranged from 4 to 7%. Additional measurements of the receiver efficiency were performed in September, using α Acq, ϵ Peg, α Peg, and β And, with the following results:

<u>Date</u>	<u>Conversion efficiency (%)</u>	<u>Comments</u>
September 21	0.6	
September 23	0.7	slightly hazy
September 24	0.4	hazy
September 26	0.2	dew on 1.5-m mirror
September 29	1.4	

The values were less than those measured earlier, partly because of the sky conditions. Equation (4) gives the true value of T only when the sky is perfectly clear; otherwise, the value is too large. A second reason for the lower values is the fact that the aluminum coating on the 1.5-m mirror deteriorates with time. (It is replaced every October.)

The lunar background noise was measured on December 12 with a 9-nm filter in place. If the measured average interelectron intervals are multiplied by $9/1.2 = 7.5$ to give corresponding values for the 1.2-nm filter, we have the results shown in Table 6.

Table 6. Lunar background noise.

Field stop		Interelectron interval		
Number	Diameter (arcsec)	Dark side (μ s)	Terminator (μ s)	Bright side (μ s)
1	4	70	30	2
2	6	30	15	1
3	10	8	4	0.2
4	25	2	1	0.04

2.8 Operation and Calibration

Figure 20 shows the locations of the retroreflectors on the moon, along with prominent, well-defined features suitable for offset guiding. The coordinates of these points are listed in Table 7. During the program, returns were obtained with direct guiding from the Apollo 15 reflector (the largest one) only; however, the system was designed and calibrated for offset guiding on any one of the four retroreflectors.

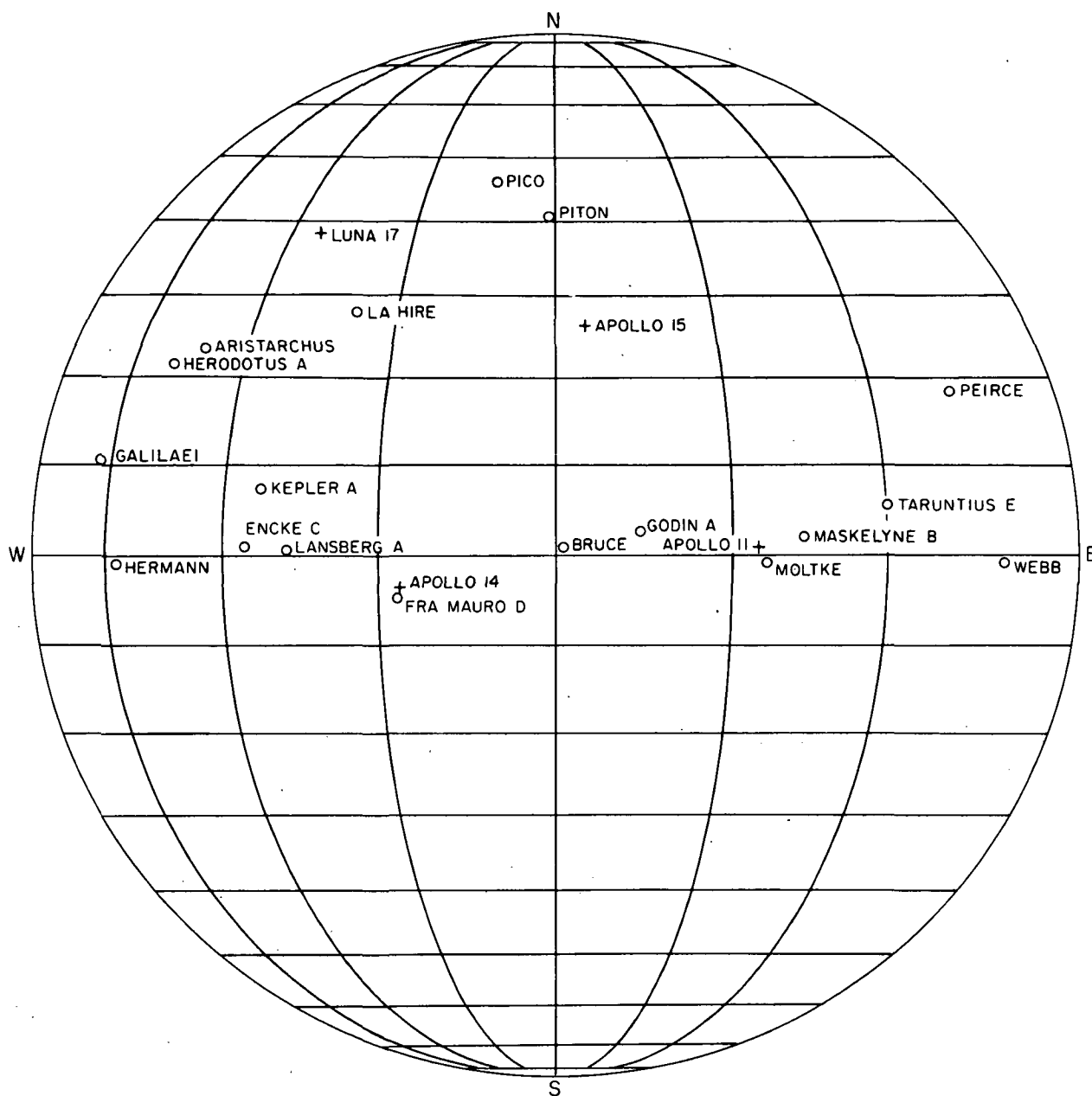


Figure 20. Locations of retroreflectors and prominent lunar features for offset guiding.

Table 7. Lunar coordinates of the four retroreflectors on the moon and the prominent features used for offset guiding.

	Longitude	Latitude
<u>Retroreflectors</u>		
Luna 17	34°58'W	38°19'N
Apollo 14	17 28 W	3 40 S
Apollo 15	3 40 E	26 05 N
Apollo 11	23 29 E	0 38 N
<u>Guiding features</u>		
Galilaei	62°46'W	10°36'N
Hermann	57 19 W	0 52 S
Herodotus A	52 04 W	21 28 N
Aristarchus	47 35 W	23 42 N
Encke C	36 24 W	0 40 N
Kepler A	36 07 W	7 07 N
Lansberg A	31 05 W	0 11 N
La Hire	25 23 W	27 35 N
Fra Mauro D	17 35 W	4 46 S
Pico	8 48 W	45 39 N
Piton	1 08 W	40 32 N
Bruce	0 24 E	1 05 N
Godin A	9 41 E	2 43 N
Moltke	24 12 E	0 34 S
Maskelyne B	28 54 E	2 00 N
Taruntius E	40 13 E	5 33 N
Peirce	53 15 E	18 14 N
Webb	59 56 E	0 56 S

The coordinates of the transmitting and receiving units were taken to be the intersections of the respective polar and declination axes. They were measured by SAO in 1971 and reported as follows by Mr. Antanas Girnius in the North American Datum:

	<u>Transmitter</u>	<u>1.5-m Telescope</u>
Longitude	288°26'36"297	288°26'30"683
Latitude	42°30'25"435	42°30'18"979
Height (above mean sea level)	180.409 m (591.894 ft)	184.720 m (606.037 ft)

The coordinates are based on the nearest U.S. Coast and Geodetic Survey control (triangulation station "Harvard, 1937-MGS" and a bench mark on the southeast pier of the old fire tower).

The above values were converted to the following set of geocentric coordinates, used by Dr. J. G. Williams of the Jet Propulsion Laboratory (JPL) and Dr. Mulholland for the computation of predictions and residuals:

<u>Transmitter</u>	<u>1.5-m Telescope</u>
$\psi = 42^{\circ}18'55"938$	$42^{\circ}18'49"485$
$\lambda_E = 288^{\circ}26'38"084$	$288^{\circ}26'32"469$
$R = 6.368\,563\,8\text{ Mm}$	$6.368\,568\,8\text{ Mm}$

Ellipsoid parameters: $a = 6.378\,155\text{ Mm}$
 $1/f = 298.255$

Collocated with 9050 Standard Earth (II)
solution (-15 m; +175 m; +182 m)

Previously, another set of coordinates, based on a slightly different geocentric correction, was used by Dr. D. H. Eckhardt of AFCRL. These geocentric coordinates are given below in rectangular form for the midpoint between the transmitting and the receiving telescopes:

$X = 1.489\,831\text{ Mm}$
 $Y = -4.467\,438\text{ Mm}$
 $Z = 4.287\,323\text{ Mm}$

Range predictions were provided by Dr. Eckhardt for 1-min intervals and by Dr. Williams for 10-min intervals. The difference between these predictions averaged 2.7 μ s on September 23. In practice, the AFCRL predictions were corrected to conform to the JPL predictions and then were set into the range-gate generator.

Dr. Eckhardt provided lunar-offset predictions. The accuracy of these predictions was confirmed in two ways – by comparing them first to predictions obtained from an independent source and then to direct measurements of the offsets between visible lunar features. The independent source was the McDonald Observatory. Dr. E. C. Silverberg gave us copies of their offset predictions for March 7 and 8, 1972, and Dr. Eckhardt computed the corresponding values for the location of the 2.7-m telescope at McDonald Observatory. The average difference for the 12 offsets compared was 2 arcsec in both right ascension and declination. Predicted offsets from AFCRL were also checked for six lunar locations on May 25 by means of the offset guider on the transmitting telescope at Agassiz Station. The measurements agreed with predictions to within 2 arcsec, the error associated with the plate-scale measurement previously made on stars.

A schematic diagram of the complete system is given in Figure 21, and a time diagram, giving the progress of the signal between transmission and reception, appears in Figure 22. Since no attempt was made to automate the system, six people were required for its operation. In the laser building, one guided the transmitting telescope and a second operated the laser and kept in telephone contact (using a direct line) with FAA's Boston Center (Nashua, New Hampshire). In the receiver building, an observer at the Newtonian focus guided the 1.5-m telescope; another monitored and set the threshold level, operated the oscilloscopes and their cameras, and restarted the counters between laser pulses; and a third set in the range-gate delay, labeled the oscilloscope photographs, and recorded the readings of the counters and other data. The sixth person observed the sky to be sure that no airplanes were in view. An intercommunication system was used to keep them in contact with one another during the ranging period.

Because the density of air traffic is high at Agassiz Station and the transmitted laser beam is intense, special arrangements were made with the FAA. A direct line

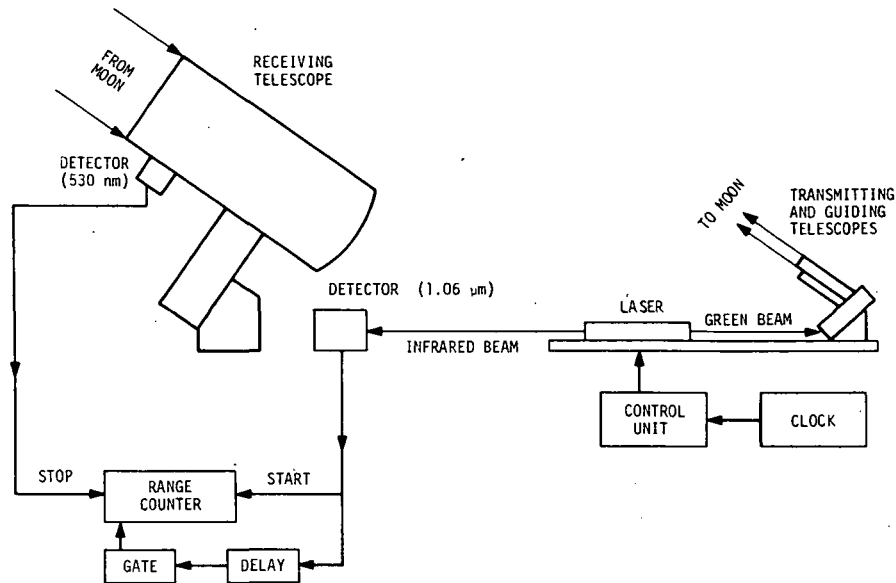


Figure 21. The lunar-ranging system.

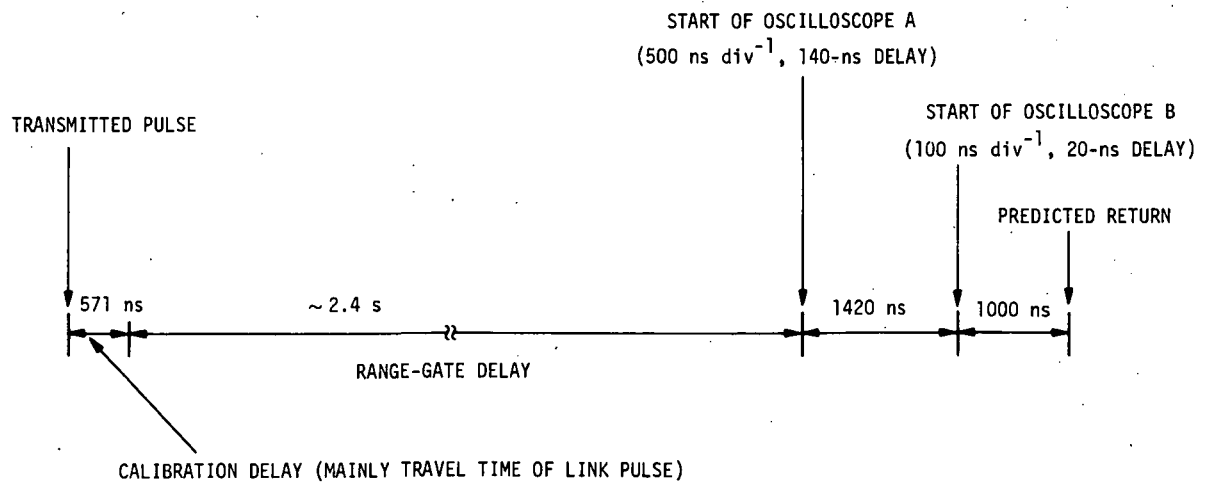


Figure 22. Time diagram for September 23, 1972.

was installed to FAA's Boston Center, a spotter for aircraft was employed during ranging periods at Agassiz, a 30° altitude limit was set, and operation was restricted to the following periods of relatively low air traffic:

Before March 14	1 to 6 a. m.
March 19 to May 26	9 p. m. to 1 a. m.
After May 26	12 midnight to 6 a. m.

These restrictions excluded most daylight hours and (according to which of the three restricted periods was in effect) limited the ranging periods to one a month: either early evening near the first quarter of the moon, or early morning near the last quarter. The high latitude of Agassiz Station also limited the hours when the moon was at a high enough altitude for ranging.

The unknown delays within a laser system are usually calibrated out by ranging on a fixed reflector whose distance is accurately known. Since at Agassiz Station there was no convenient point where a reflector visible from both the receiver and the transmitter could be set up, a variation on this scheme was devised. Instead of a fixed reflecting surface, a small scattering volume in the atmosphere was used. This procedure was possible because the separated transmitting and receiving telescopes could be positioned accurately on stars and because their respective beam spreads were each only a few arcseconds. A diagram of the triangle formed by the laser beam, the telescope's field, and the distance between the transmitter and the receiver is shown in Figure 23. The laser beam and the field of the 1.5-m telescope were directed as follows. First the laser beam was positioned to point in a plane that contained the celestial pole and a line through the receiving telescope and the transmitting telescope, by tracking a star and stopping the telescope at a previously calculated epoch. At this epoch, the hour angle to which the transmitter was pointed was $2^{\text{h}}51^{\text{m}}44.2^{\text{s}}$. A star near the equator was chosen for an intersection close to 90° with the field of the 1.5-m telescope. The receiving telescope was positioned in a direction nearly that of the celestial pole by tracking Polaris and stopping at some convenient sidereal time (ST). Then the hour angle of the telescope was increased (i. e., driven westward) by either $4^{\text{h}}56^{\text{m}}40^{\text{s}}$ or $16^{\text{h}}56^{\text{m}}40^{\text{s}}$ ST. The telescope's readout dials were sufficiently accurate for this purpose since, at the declination of Polaris, an hour-angle error of 5 s produces a pointing error of only 1 arcsec. Once the telescopes were positioned,

the laser was pulsed at reduced energy and the reading of the range counter was recorded. The calibration correction is the difference between this reading and the calculated propagation time for the path of the laser beam shown in Figure 23. The measured value of the calibration constant on September 23 was 571 ns.

201-089

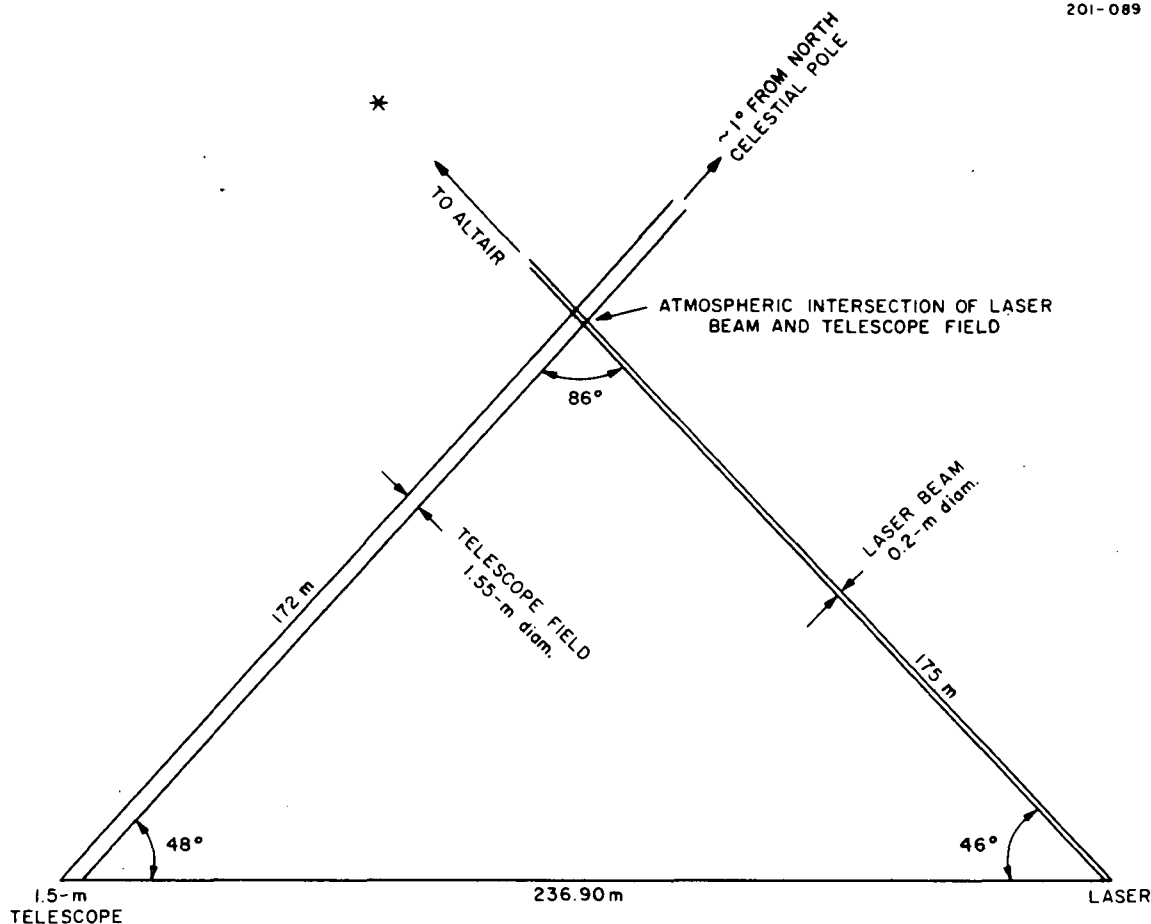


Figure 23. Diagram of the laser beam and the telescope field in the plane of their intersection (the star Altair, or some other bright star, is used to position the laser beam).

2.9 Operational Statistics

Table 8 gives the operational statistics for the system from the time it was first operational (February 1972) until the program was completed (September 1972). The second column gives the number of hours when the sky was dark and the moon was

Table 8. Operational statistics (February through September 1972).

Month	Number of hours						Clear weather and time available on 1.5-m telescope	Number of pulses	Number of returns
	Altitude of moon >30°		Altitude of moon >30° and FAA permission	Time available on 1.5-m telescope					
	Night	Day							
February	95	51	42	20	0 [*]		24	0	
March	83	68	50	24	0		0	0	
April	43	93	25	22	14		72	0	
May	26	111	19	17	6		45	2	
June	16	119	17	8	3		11	0	
July	37	117	48	21	7		49	1	
August	63	105	65	20	2		12	0	
September	78	81	61	54	6		50	6	
Total	441	745	327	186	38		263	9	

* Moon was at an altitude of 22° to 29° when laser was pulsed.

high enough in the sky for ranging. The third column shows the number of hours during which daylight ranging was possible, and the fourth, the total number of hours (predominantly nighttime) that also met FAA requirements. The fifth column gives the number of hours requested from and granted by HCO for the use of the 1.5-m instrument. The number of times the laser was pulsed and the number of returns obtained are presented in the final two columns. The interpulse interval was 10 min in February and 5 min thereafter; the total operating time for the 8-month period was 24 hours. Over the entire ranging period, 1 return was obtained for every 29 transmitted pulses. During the final month, September, the ratio was 1:8, and on September 23, it was 1:5. On this night, the receiver efficiency was low by about a factor of 4, presumably because the mirror of the 1.5-m telescope needed to be realuminized, because the energy of the laser was about half its rated value, and because the atmospheric transmission was about half the clear-sky value. Hence, the expected average signal strength per pulse was not the 15 photoelectrons given in Section 2.4, but $0.25 \times (0.5)^2 \times 15 = 1$ photoelectron for an altitude of 30° and a range of 384 Mm.

Further information on the nine returns is given in Table 9. The altitude and distance of the moon varied significantly from the values of 30° and 384 Mm used in calculating the average signal strength of 15 photoelectrons. For the positions of the moon corresponding to the epochs of the returns in Table 9, the calculated returns range from 12 to 32 photoelectrons. The measured signal strengths were obtained from the pulse amplitudes of the oscilloscope photographs. Except for the single-electron returns, these photographs are reproduced in Figure 24.

2.10 Data Handling

Because the data rate of the system at Agassiz Station was low, it was possible to operate without any automation of the data handling. The range-gate-delay values were set in by hand and the counter readings copied onto data sheets from digital displays. This procedure is inefficient and should be modified if the system is moved to a location where operation is less restricted by weather and air traffic. We will describe here the data needed to operate the system, the recording of the returns and related data while lunar ranging was in progress, and the processing of the returns for use in a lunar ephemeris. The system configuration of September 1972 will be assumed. The procedure was somewhat simpler in previous months when only one oscilloscope and one counter were used.

Table 9. Summary of returns. (All returns were from the Apollo 15 retroreflector, and all were with the system in the direct-guiding mode.)

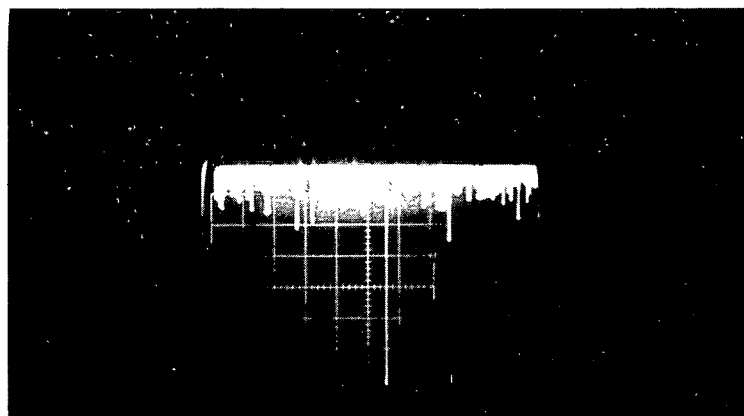
Epoch (Universal Time)	Altitude of the moon (deg)	Distance of the moon (Mm)	Measured signal strength (photoelectrons)	Background noise interval (μ s)
May 23 2 ^h 58 ^m	33	398	3	55
May 24 3 37	28	400	6	36
July 31 8 42	57	365	3	18
September 23 6 36	43	360	2	15
September 23 7 01	40	360	2	15
September 23 7 06	40	360	1	0.13
September 23 7 31	36	360	1	0.13
September 23 7 52	32	361	2	15
September 23 8 12	30	361	1	0.13

$2^h_{58}m$



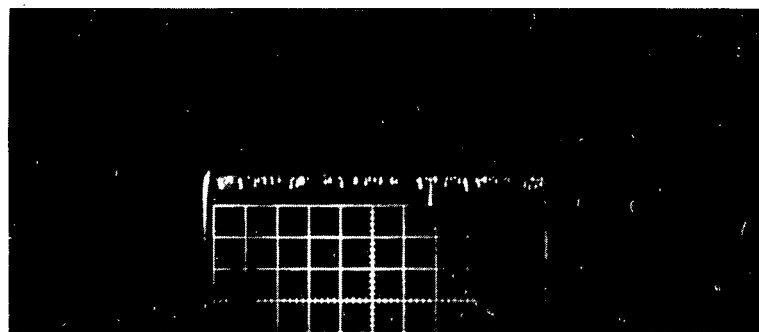
May 23, 1972 Horizontal scale: $1 \mu s \text{ div}^{-1}$

$3^h_{37}m$



May 24, 1972 Horizontal scale: $2 \mu s \text{ div}^{-1}$

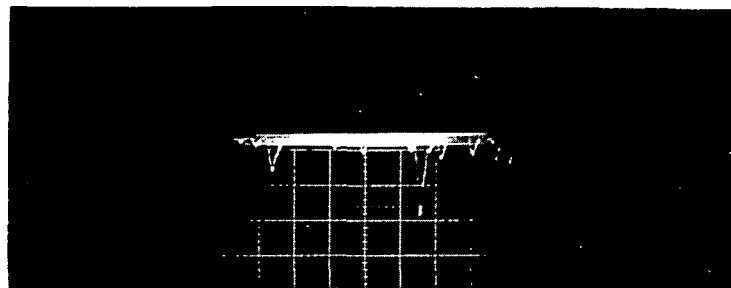
$8^h_{42}m$



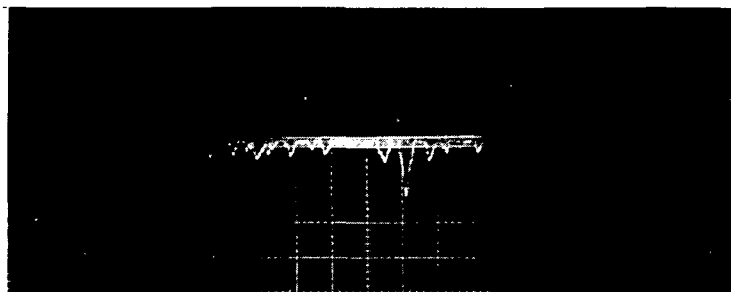
July 31, 1972 Horizontal scale: $2 \mu s \text{ div}^{-1}$

Figure 24. Photographs of returns with signal strengths of 2 photoelectrons or more.

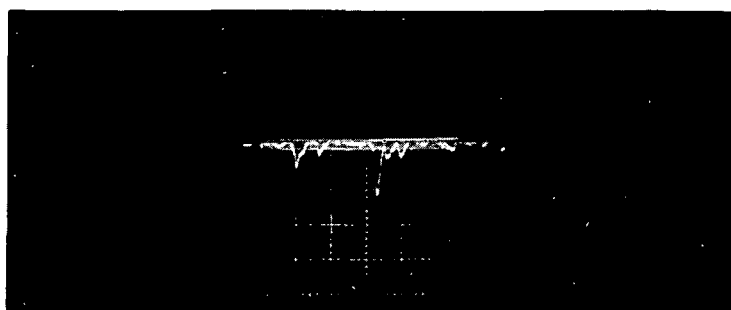
6^h36^m



7^h01^m



7^h52^m



September 23, 1972 Horizontal scale: 100 ns div⁻¹

Figure 24 (Cont.)

The collection of the information needed to operate the system was started by running a program that computes the altitude of the moon to within an accuracy of a degree or two for each hour of the day over a period of several months. From these results, nights were selected when the moon's altitude was greater than 30° and the FAA conditions for low air traffic were met. Telescope time for these nights was then requested from HCO. Before the beginning of each monthly observing period, a more accurate ephemeris of the moon (the JPL ephemeris) was used to compute the following information at hourly intervals:

- A. The sidereal time, which was used for star settings in the range calibration.
- B. The moon's hour angle and declination, used to place the moon within the fields of the transmitting and the receiving telescopes.
- C. The moon's altitude, which was used in satisfying the FAA requirements and in making the atmospheric correction to the range-counter reading.
- D. The hour-angle and declination rates of the moon (in arcsec s^{-1}), which were available, but seldom used, in setting up the transmitting telescope.
- E. The hour-angle rate setting for the 1.5-m telescope in the particular units appropriate to its drive system.

Other data required for the operation of the system were supplied by Dr. Eckhardt, who provided at no charge both two-way transit times to the retroreflectors on the moon and offsets between these retroreflectors and selected lunar features. His two-way transit times (computed from an ephemeris of the Massachusetts Institute of Technology), at intervals of 1 min, were used (after being modified as described below) to set the range-gate generator. The offsets were available for positioning the transmitting and receiving telescopes to a retroreflector on the dark side of the moon. However, once it was found that the system had sufficient background discrimination when directed toward a fully illuminated retroreflector, offsetting was seldom used. Transit-time predictions were also provided at no charge by Dr. Williams. According to various members of the LURE group, these predictions were accurate to a few tenths of a microsecond. Since they were available only at 10-min intervals, they were used to modify the AFCRL predictions, available at 1-min intervals but differing from the JPL predictions by as much as $2 \mu\text{s}$ or more.

During operation, data were recorded at both the transmitting and the receiving sites. The following were recorded at the transmitter:

- A. The lunar retroreflector that was ranged on.
- B. The guiding feature on the moon.
- C. The epoch of each laser pulse.
- D. The time difference between the station clock and Loran C.
- E. The voltage inputs to the laser's Q-switch, oscillator, and amplifier.
- F. An estimate of the laser energy.
- G. The pulse duration.
- H. Comments on the guiding, atmospheric seeing, and other matters affecting the system's operation.

At the receiver, the following data were written down:

- A. The lunar retroreflector that was ranged on.
- B. The guiding feature on the moon.
- C. The epoch.
- D. The reading of the 0.1-ns range counter.
- E. The reading of the 10-ns counter that measured the range-gate delay.
- F. The range window (almost always set at 200 μ s).
- G. The gain of the video amplifiers.
- H. The video attenuation.
- I. The horizontal and vertical settings of oscilloscopes A and B.
- J. The DC background current of the photomultiplier tube.
- K. The PMT voltage.
- L. The field-stop setting.
- M. Comments on guiding and operation of the receiving system.
- N. The ambient temperature, humidity, wind speed, and atmospheric pressure.

The oscilloscope photographs were also marked with the proper epoch.

When the ranging period was over, time intervals from the start of the sweep were measured for all the single-electron pulses that appeared on the photographed traces of oscilloscope B. To these values were added the readings of the 10-ns counter and the delay between the output of the range-gate generator and the start of sweep B. Once these computations were performed, the oscilloscope readings were processed, along with the readings of the 0.1-ns counter, in the manner described below.

A computer program was used to perform the following operations on the ranging readings from the 0.1-ns counter and oscilloscope B:

- A. To apply the atmospheric correction.
- B. To compute the residual from the JPL predictions.
- C. To punch the data on cards in the COSPAR format (Mulholland, 1972).

The atmospheric correction is based on an expression given by Hopfield (1971, eq. (11), p. 359), which shows that the range correction ΔR for a vertical path is proportional to the surface pressure. The proportionality constant she gives is for dry air at radio frequencies. At the frequency of the laser, the effect of humidity is very small; however, the proportionality constant is different from that at radio frequencies. Hence, a new proportionality constant was derived for a wavelength of 530 nm by use of equation (42) from Owens (1967). A trigonometric factor was also included for cases when the moon was at a zenith angle Z . The resulting expression is

$$\Delta t = 0.01612P \sec Z, \quad (7)$$

where Δt is the two-way atmospheric correction (in ns) to be subtracted from the range reading, P is the surface pressure (in mb), and Z is the zenith angle of the moon.

Residuals for the returns obtained with the system are given in Table 10. The JPL residuals are those calculated at SAO from the JPL predictions. The residuals from the University of Texas were supplied by Dr. Mulholland. The returns in May and

July were distinguished from noise by the large amplitude of the received signal; those in September were obtained by Dr. Mulholland from the fact that their residuals lay on a line whose slope with time was reasonable.*

Table 10. Residuals for the laser returns.

	Epoch (Universal Time)	Type of return	Residual (μ s)	
			JPL	University of Texas
May 23	2 ^h 58 ^m 00. ^s 001238	counter	+0.966	-1.052
May 24	3 37 00.002056	counter	+1.731	-0.140
July 31	8 42 00.001064	counter	+0.806	+0.833
September 23	6 36 00.000011	counter	-0.138	0.000
September 23	6 36 00.000011	oscilloscope	-0.115	+0.023
September 23	7 01 00.000011	counter	-0.134	+0.019
September 23	7 01 00.000011	oscilloscope	-0.117	+0.036
September 23	7 06 00.000011	oscilloscope	-0.136	+0.020
September 23	7 31 00.000011	oscilloscope	-0.140	+0.029
September 23	7 51 59.997992	counter	-0.153	+0.029
September 23	7 51 59.997992	oscilloscope	-0.140	+0.042
September 23	8 11 59.997992	oscilloscope	-0.150	+0.038

* According to Dr. Williams, a slope of 1 ns min^{-1} is equivalent to an error in station position of about 1 arcsec in longitude, which is 23 m at a latitude of $42^\circ 5'$. The slope for the counter returns was $+0.35 \text{ ns min}^{-1}$; that for the oscilloscope returns, $+0.22 \text{ ns min}^{-1}$. See Figure 25.

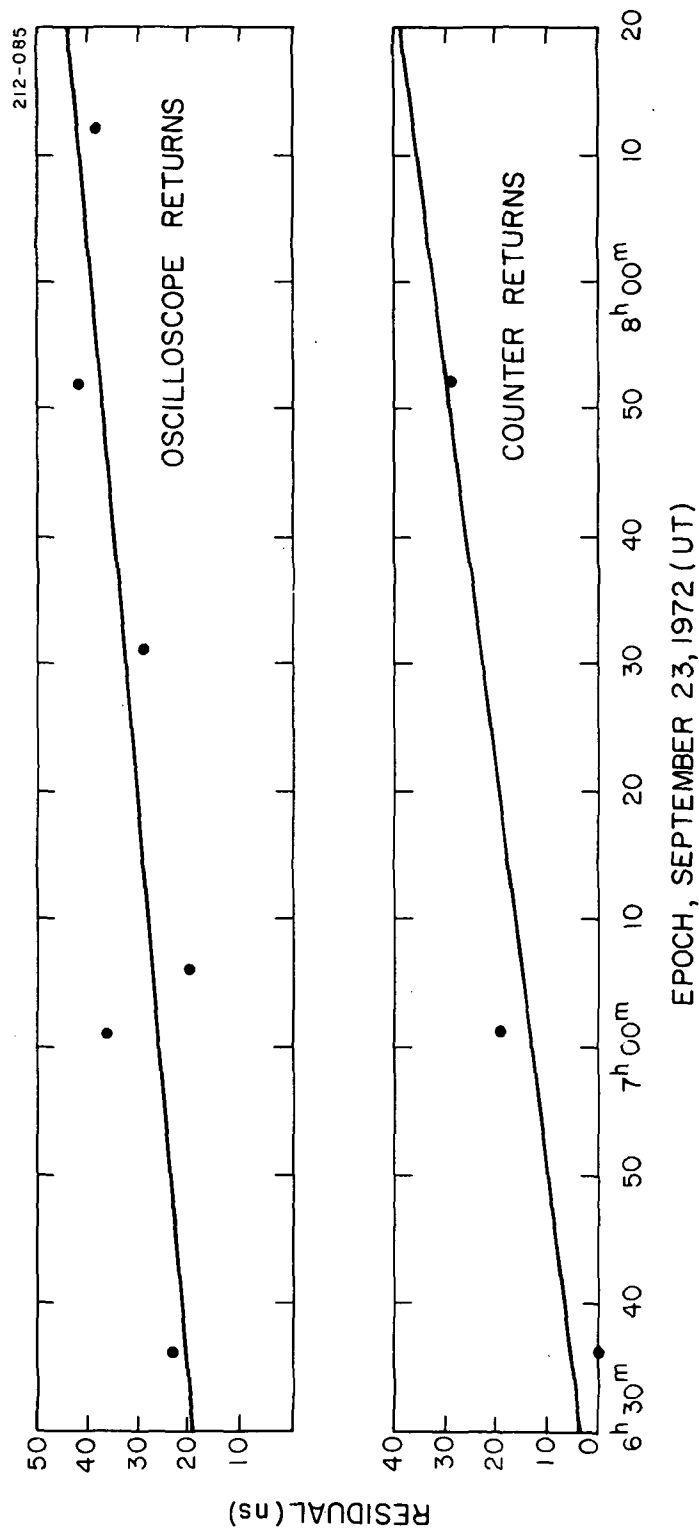


Figure 25. Residuals (from the University of Texas) as a function of epoch.

3. ACKNOWLEDGMENTS

This program received a substantial amount of support at no cost from various sources. Personal time was donated by SAO staff members in the construction of the building for the laser and the transmitting telescope. Significant amounts of electronic equipment, such as time-interval counters, oscilloscopes, and a portable clock, were borrowed from SAO's satellite-tracking program. Prof. W. Liller of Harvard College Observatory scheduled observing time on the 1.5-m telescope at Agassiz Station and M. Mattei of HCO operated this instrument for tests and for lunar ranging. Dr. J. G. Williams of JPL and Dr. W. H. Eckhardt of AFCRL computed the lunar-range predictions for Agassiz Station; in addition, Dr. Eckhardt provided lunar-offset values. Drs. C. O. Alley and E. C. Silverberg of the LURE team gave us complete details on the operation of the system at McDonald Observatory and made many helpful suggestions. Dr. J. G. Baker of HCO was particularly generous with his time in consulting on difficult optical problems. Dr. J. D. Mulholland of the University of Texas both analyzed our returns and made helpful suggestions. Mr. J. Campbell and Mr. R. Gale of the FAA's Boston Center were most cooperative in making arrangements to have the FAA monitor air traffic in the vicinity of Agassiz Station when laser ranging was in progress.

4. REFERENCES AND BIBLIOGRAPHY

AERONAUTICAL CHART AND INFORMATION CENTER

Lunar Charts. Aeronautical Chart and Information Center, United States
Air Force, St. Louis, Missouri.

ALLEY, C. O.

1971. Laser ranging to the moon. Presented at Open Meeting of Working Group 1,
XIVth COSPAR Meeting, Seattle, Washington.

ALLEY, C. O., BENDER, P. L., DICKE, R. H., FALLER, J. E.,
FRANKEN, P. A., PLOTKIN, H. H., and WILKINSON, D. T.

1965. Optical radar using a corner reflector on the moon. *Journ. Geophys. Res.*,
vol. 70, pp. 2267-2269.

CARTER, W. E., ECKHARDT, D. H., ROBINSON, W. G.

1972. AFCRL lunar laser instrumentation status report. In Space Research XII,
ed. by S. A. Bowhill, L. D. Jaffe, and M. J. Rycroft, Akademie-Verlag,
Berlin, pp. 177-186.

CLARKE, A. M.

1971. Ocular hazards. In Handbook on Lasers, ed. by R. J. Pressley, The
Chemical Rubber Co., Cleveland, pp. 3-10.

EASTMAN KODAK CO.

1971. Neutral density attenuators. Eastman Kodak Co., Pamphlet P-114, p. 3.

FALLER, J. E., and WAMPLER, E. J.

1970. The lunar laser reflector. *Sci. Amer.*, vol. 222, pp. 38-49.

GOODMAN, J. W.

1965. Some effects of target-induced scintillation on optical radar performance.
Proc. IEEE, vol. 53, pp. 1688-1700.

HAGEN, W. F.

1969. Diffraction-limited high-radiance, Nd-glass laser system. *Journ. Appl.
Phys.*, vol. 40, pp. 511-516.

HAGEN, W. F., and MAGNANTE, P. C.

1969. Efficient second-harmonic generation with diffraction-limited and high-
spectral-radiance Nd-glass lasers. *Journ. Appl. Phys.*, vol. 40,
pp. 219-224.

HOPFIELD, H. S.

1971. Tropospheric effect on electromagnetically measured range: prediction from surface weather data. *Radio Sci.*, vol. 6, pp. 357-367.

KANTORSKI, J. W., and YOUNG, C. G.

1963. Diffraction limited, single mode glass laser (abstract). *Journ. Opt. Soc. Amer.*, vol. 53, p. 1339.

KAULA, W. M.

1962. Celestial geodesy. In Advances in Geophysics, ed. by H. E. Landsberg and J. Van Mieghem, Academic Press, New York, vol. 29, pp. 191-293.
1970. (Chairman) The Terrestrial Environment: Solid-Earth and Ocean Physics. Report of a Study at Williamstown, Mass., NASA CR-1579.

KOKURIN, Yu. L., KURBASOV, V. V., and SUKHANOVSKIY, A. N.

1972. Lunar laser ranging experiment. Presented at Open Meeting of Working Group 1, XIVth COSPAR Meeting, Seattle, Washington.

KUIPER, G. P.

1960. Orthographic Atlas of the Moon. University of Arizona Press, Tucson.

LEHR, C. G., CRISWELL, S. J., OUELLETTE, J. P., SOZANSKI, P. W., MULHOLLAND, J. D., and SHELUS, P. J.

1973. Laser transit-time measurements between earth and moon with a transportable system. Submitted to *Science*.

LEHR, C. G., OUELLETTE, J. P., SOZANSKI, P. W., WILLIAMS, J. T., CRISWELL, S. J., and MATTEI, M.

1973. Lunar range measurements with a high-radiance, frequency-doubled, neodymium-glass laser system. *Appl. Opt.*, Letter to the Editor, in press.

LEHR, C. G., PEARLMAN, M. R., and MONJES, J. A.

1972. The SAO lunar laser. In Space Research XII, ed. by S. A. Bowhill, L. D. Jaffe, and M. J. Rycroft, Akademie-Verlag, Berlin, pp. 197-204.

LEHR, C. G., PEARLMAN, M. R., MONJES, J. A., and HAGEN, W. F.

1972. Transportable lunar-ranging system. *Appl. Opt.*, vol. 11, pp. 300-304.

LEHR, C. G., PEARLMAN, M. R., WOLF, M. R., MONJES, J. A., and HAGEN, W. F.

1971. A high-radiance laser system for lunar ranging. In Optical Tracking Systems, ed. by J. G. Muckleberger and E. D. Miller, SPIE Seminar Proc., vol. 23, pp. 163-166.

MARQUET, L. C.

1971. Transmission diffraction grating attenuator for analysis of high power laser beam quality. Appl. Opt., vol. 10, pp. 960-961.

MITCHELL, R. I., and JOHNSON, H. L.

1969. Thirteen-color narrow-band photometry of one thousand bright stars. Lunar and Planetary Laboratory, University of Arizona, Comm. No. 132, vol. 8, part 1, 49 pp.

MULHOLLAND, J. P.

1972. Proposed standards for distribution and documentation of lunar laser ranging data. COSPAR Information Bull. No. 61, March, pp. 47-55.

NATIONAL AERONAUTICS AND SPACE ADMINISTRATION

1972. Earth and Ocean Physics Applications Program. National Aeronautics and Space Administration, Washington, D.C., September, 2 vols.

ORSZAG, A., and CALAMME, O.

1971. La station télémétrie laser de l'Observatoire du Pic du Midi. In Bulletin du Groupe de Recherches de Géodésie Spatiale No. 1, ed. by J. C. Husson, pp. 75-85.

OWENS, J. C.

1967. Optical refractive index of air: dependence on pressure, temperature, and composition. Appl. Opt., vol. 6, pp. 51-59.

REILLY, J. P.

1972. Single-mode operation of high-power pulsed N_2/CO_2 laser. IEEE Journ. Quant. Electron., vol. QE-8, pp. 136-139.

SIDGWICK, J. B.

1971. Amateur Astronomer's Handbook. Faber & Faber, London, 577 pp.

SILVERBERG, E. C., and CURRIE, D. G.

1972. A description of the lunar ranging station at McDonald Observatory. In Space Research XII, ed. by S. A. Bowhill, L. D. Jaffe, and M. J. Rycroft, Akademie-Verlag, Berlin, pp. 219-233.

SMULLIN, L. D., and FIOCCO, G.

1962. Project Luna See. Proc. IRE, vol. 50, pp. 1703-1704.

TACHIBANA, A., YAMAMOTO, Y., TAKATSUJI, M., MURASAWA, K., and KOZAI, Y.

1972. A preliminary system of lunar laser ranging. In Space Research XII, ed. by S. A. Bowhill, L. D. Jaffe, and M. J. Rycroft, Akademie-Verlag, Berlin, pp. 187-195.

WAYNANT, R. W., CULLOM, J. H., BASIL, I. T., and BALDWIN, G. D.

1965. Beam divergence measurement of Q-switched ruby lasers. *Appl. Opt.*, vol. 4, pp. 1648-1651.

YOUNG, C. G.

1969. Glass lasers. *Proc. IEEE*, vol. 57, pp. 1267-1289.

5. LIST OF PROGRESS REPORTS

Laser System of Extended Range, Contract NASW-2014

No. 1	November 1, 1969 through April 30, 1970	May 1970
No. 2	May 1 through July 31, 1970	August 1970
No. 3	August 1 through December 31, 1970	January 1971
No. 4	January 1 through April 30, 1971	May 1971
No. 5	May 1 through December 31, 1971	January 1972